This document was prepared in conjunction with work accomplished under Contract No. DE-AC09-96SR18500 with the U.S. Department of Energy.

Hybrid Sulfur flowsheets using PEM electrolysis and a bayonet decomposition reactor

Maximilian B. Gorensek*, William A. Summers

Savannah River National Laboratory, Aiken, SC 29808 USA

Abstract

A conceptual design is presented for a Hybrid Sulfur process for the production of hydrogen using a high-temperature nuclear heat source to split water. The process combines proton exchange membrane-based SO_2-depolarized electrolyzer technology being developed at Savannah River National Laboratory with silicon carbide bayonet decomposition reactor technology being developed at Sandia National Laboratories. Both are part of the US DOE Nuclear Hydrogen Initiative. The flowsheet otherwise uses only proven chemical process components. Electrolyzer product is concentrated from 50 wt% sulfuric acid to 75 wt% via recuperative vacuum distillation. Pinch analysis is used to predict the high-temperature heat requirement for sulfuric acid decomposition. An Aspen Plus™ model of the flowsheet indicates 340.3 kJ high-temperature heat, 75.5 kJ low-temperature heat, 1.31 kJ low-pressure steam, and 120.9 kJ electric power are consumed per mole of H_2 product, giving an LHV efficiency of 35.3% (41.7% HHV efficiency) if electric power is available at a conversion efficiency of 45%.

Keywords: Hybrid Sulfur, Hydrogen, SO_2-depolarized, Proton Exchange Membrane, Electrolyzer, Efficiency, Silicon Carbide, Bayonet, High-temperature, Decomposition, Reactor, Nuclear, Pinch Analysis, Aspen Plus™, Flowsheet, Model, Vacuum Distillation

* Corresponding author. Tel.: (803) 725-1314; Fax: (803) 725-8829;
E-mail address: maximilian.gorensek@srnl.doe.gov

1. Introduction

The push for a Hydrogen Economy in the United States (U.S.) is largely driven by the desire to replace fossil-based, hydrocarbon fuels for transportation, particularly in automobiles. Fuel cell-powered vehicles fueled with hydrogen (H_2) emit no greenhouse gases – only water – and their fuel can be derived from greenhouse gas-neutral, non-fossil energy sources. If the U.S. should transition to a Hydrogen Economy, the National Academies have projected that the H_2 needed to fuel all U.S. light-duty vehicles alone will reach 110 MMt/yr by 2050 [1]. This has a power equivalent of 450 GW_{th} and represents a twelve-fold increase over current U.S. H_2 consumption, which is primarily for industrial needs. For comparison, the average U.S. electric power demand in 2007 was 446 GW_e [2]. Other uses for H_2 (heavy-duty vehicles, fertilizer and chemicals manufacturing, distributed power, etc.) could easily double the total demand over that for light-duty vehicles. The energy required to make so much H_2 would be comparable to that needed for electric power generation. As a result, it will necessarily rely on multiple primary energy sources, such as fossil fuels (with carbon dioxide sequestration), renewable energy coupled with electrolysis, and nuclear water-splitting, in much the same way that the U.S. electricity supply does currently.

The U.S. Department of Energy's Office of Nuclear Energy, Science & Technology (DOE-NE) has established the Nuclear Hydrogen Initiative (NHI) to develop technologies that can be coupled with next generation nuclear reactors to produce H_2 on such a massive scale. Thermochemical water-splitting cycles are leading contenders within the NHI program because they have the potential for higher efficiencies than water electrolysis with more favorable scale-up characteristics.

Research programs world-wide recognize sulfur-based thermochemical cycles as high priority candidates for research and development. The NHI has identified the Hybrid Sulfur (HyS) and the Sulfur-Iodine (SI) cycles as the two first priority baseline cycles. Both have the potential for significantly higher thermal efficiency than water electrolysis, and both have been demonstrated at the laboratory scale to confirm performance characteristics. The two cycles share a common, high-temperature reaction step – the catalytic, vapor phase thermal decomposition of sulfuric acid (H_2SO_4).

The Savannah River National Laboratory (SRNL) has been tasked by the NHI with developing the SO_2-depolarized electrolyzer (SDE), which distinguishes the HyS from other sulfur cycles. As part of this work, SRNL has also prepared conceptual designs of HyS processes that use SDEs of the type being developed and that are powered by an advanced nuclear reactor heat source. The purpose of this manuscript is to communicate the results of the latter task to date.

2. Background

2.1 The Hybrid Sulfur cycle

The HyS cycle was first proposed by Brecher and Wu [3] at Westinghouse Electric Corp., where it was extensively developed in the 1970s and 1980s [4,5,6]. As a result, it has also come to be known as the Westinghouse process [7]. HyS is one of the simplest thermochemical cycles, comprising only two reaction steps and having only fluid reactants. The "hybrid" designation acknowledges the electrochemical nature of one of the reaction steps, which requires that electric as well as thermal energy be supplied to the process. It is a sulfur cycle because it

entails sulfur oxidation and reduction. In fact, sulfur is the only element in the cycle other than H_2 and oxygen (O_2).

A simple schematic of the HyS cycle that illustrates the two reaction steps and how they interact to split water is shown in Fig. 1. The first reaction step,

$$H_2SO_4(aq) \rightarrow H_2O(g) + SO_2(g) + \tfrac{1}{2}O_2(g) \quad (1)$$

common to all sulfur cycles, is, in reality, the result of two separate reactions. As H_2SO_4 is vaporized and superheated, it spontaneously decomposes into water (H_2O) and sulfur trioxide (SO_3),

$$H_2SO_4(aq) \rightarrow H_2O(g) + SO_3(g)\,. \quad (1a)$$

Further heating the vapor to high temperatures (>800 °C, 1073 K) in the presence of a catalyst drives the endothermic decomposition of SO_3 into O_2 and sulfur dioxide (SO_2),

$$SO_3(g) \rightarrow SO_2(g) + \tfrac{1}{2}O_2(g) \quad (1b)$$

After O_2 is removed as a co-product, the SO_2 and H_2O are combined with make-up H_2O (and recycled H_2SO_4) and fed to the anode of an electrolyzer, where the second reaction takes place. This is the SO_2-depolarized electrolysis of water,

$$SO_2(aq) + 2H_2O(l) \rightarrow H_2SO_4(aq) + H_2(g) \quad (2)$$

illustrated in Fig. 2. SO_2 is electrochemically oxidized at the anode to form H_2SO_4, protons and electrons.

$$SO_2(aq) + 2H_2O(l) \rightarrow H_2SO_4(aq) + 2H^+ + 2e^- \quad (2a)$$

The protons are conducted across the electrolyte separator to the cathode, where they recombine with the electrons, which pass through an external circuit, to form H_2.

$$2H^+ + 2e^- \rightarrow H_2(g) \quad (2b)$$

The net result is H_2SO_4 production at the anode and H_2 production at the cathode. H_2SO_4 is recycled to the high-temperature decomposition step to complete the cycle, while H_2 is removed as the principal product.

What makes the HyS cycle attractive is the standard cell potential for SO_2-depolarized electrolysis, which is only -0.158 V at 25 ºC (298 K) in water [8,9]. The reversible potential increases in magnitude to -0.243 V if SO_2 is dissolved to saturation at 1 bar total pressure in a 50-wt% H_2SO_4-H_2O solution, the most likely anolyte[1]. This means that the SDE will consume much less electricity per mole of H_2 product than water electrolysis, which has a reversible cell potential of -1.229 V at 25 °C (298 K) [8,9], and which is an obvious H_2 production alternative.

In reality, water electrolyzers operate at cell potentials of -1.7 to -2.0 V when economically reasonable current densities are maintained. Ohmic losses and electrode overpotentials are responsible for this voltage increase. Likewise, SDEs in which the SO_2 is dissolved in 50 wt% H_2SO_4 are expected to operate with cell potentials significantly greater than -0.243 V at practical current densities.

In 1981, Lu et al. [10] predicted that cell potentials of -0.45 to -0.75 V could be obtained at current densities of 100 to 400 mA/cm^2 for properly designed and optimized SDEs. Recent experience with proton exchange membrane (PEM) SDE development at SRNL suggests that cell potentials of -0.6 V should be attainable at practical current densities with higher operating temperatures (≥100 °C, 373 K) and pressures (≥10 bar). The target of SRNL's SDE development program is, in fact, a potential of -0.6 V at a current density of 500 mA/cm^2.

Therefore, it is anticipated that the HyS SDE will operate with a cell potential significantly lower than that of a conventional alkaline electrolyzer.

[1] Correction for nonstandard condition calculated using the Nernst equation [9], with species activities obtained from the Mixed Solvent Electrolyte model in OLI Systems, Inc.'s OLI Engine 7.0.

2.2 Energy considerations

A key benchmark against which the HyS cycle will ultimately be judged is the use of conventional nuclear power generation coupled with water electrolysis. Both are proven technologies that could be deployed almost immediately, although this would require a large scale-up from existing water electrolysis plants. In order for the more complex HyS cycle to be competitive with the simpler, direct electrolysis of water, it needs to provide a significant advantage in terms of higher process thermal efficiency. No capital cost estimates were included in this study, but some general observations can be made about the competing hydrogen production options.

If the HyS plant has a higher thermal efficiency, it will require a smaller nuclear heat source than the water electrolyzer plant. Since the nuclear heat source is expected to be the most capital intensive portion of the plant, the nuclear-HyS plant could be expected to have a lower total capital investment (nuclear plant plus hydrogen plant) and a resulting lower hydrogen production cost. This could be offset, however, if there is an overwhelming difference in the capital cost between the two hydrogen production processes, or if the efficiency difference is minor. Further studies will investigate this issue and the trade-offs between plant efficiency and capital cost. Qualitatively, however, it is clear that the HyS plant efficiency must be substantially better than the water electrolysis plant efficiency.

Existing nuclear power plants generate electricity using either a boiling water reactor (BWR) or pressurized water reactor (PWR) combined with a steam-driven Rankine cycle power conversion unit (PCU). The maximum temperature of the steam is typically less than 315 °C (588 K), and the overall thermal-to-electric conversion efficiency for the power plant is

approximately 33%. H_2 can be produced via water electrolysis with an electric-to-lower heating value (LHV) conversion efficiency of 62 to 68% [11,12] [2]. Combining the two steps would allow H_2 to be produced from nuclear energy at an overall LHV efficiency of 21 to 23%. This represents a heat requirement of 4.5 MW_{th} of fission heat to make a one-MW_{th} equivalent of H_2 (in terms of fuel value) using conventional nuclear power plant (BWR or PWR) technology.

The overall efficiency could be increased by utilizing an advanced Generation IV nuclear reactor system, such as the high-temperature gas-cooled reactor (HTGR), which has a higher thermal-to-electric conversion efficiency. An HTGR can produce hot helium at 850 to 950 °C (1123 to 1223 K) and be combined with a helium-driven closed-loop Brayton cycle PCU. The resulting thermal-to-electric conversion efficiency could be between 42% and 48%, depending on the exact cycle design. In that case, the overall LHV efficiency of H_2 production for an HTGR-water electrolysis hydrogen plant could be as high as 33%, or 3.0 MW_{th} of fission heat per one-MW_{th} equivalent of H_2.

The HyS plant will require both electricity for the SDE and thermal energy for acid decomposition. In order for the HyS plant to exceed the nuclear-electrolysis plant efficiency, the thermal energy required to effect the decomposition of H_2SO_4 will need to be substantially less than the thermal equivalent of the difference in cell potentials between the SDE and the water electrolyzer. The electric power requirement for the HyS electrolysis step is 116 kJ/mol H_2 product, based on an assumed SDE cell potential of -0.6 V. If a conventional BWR/PWR nuclear reactor is used to produce this electricity, the thermal equivalent is 352 kJ/mol H_2. On the other hand, if an HTGR power plant operating with an assumed thermal-to-electric

[2] Alkaline electrolysis can produce H_2 at pressure using 4.8 kWh/Nm^3 [11], while PEM electrolysis requires about 4.4 kWh/Nm^3 [12]. These figures are equivalent to 387 and 355 kJ_e/mol H_2, respectively. The LHV, or lower heating value, of H_2 is 242 kJ/mol. An LHV efficiency of 68% implies that 242/0.68 = 356 kJ of electric energy is needed to make 1 mol H_2. For comparison, the HHV, or higher heating value, of H_2 is 286 kJ/mol, so an H_2 LHV efficiency of 68% is equivalent to an H_2 HHV efficiency of 80.3%.

conversion efficiency of 45% is used instead, the thermal equivalent of the power for the SDE is only 258 kJ/mol H_2. Table 1 shows the calculation for "allowable" thermal energy use in the HyS plant compared to the water electrolysis plant.

BWR/PWR-powered water electrolysis at 22.4% overall LHV efficiency would consume 1,080 kJ of thermal energy per mol H_2 product. That leaves an allowance of as much as 1,080 kJ – 352 kJ = 728 kJ heat per mol H_2 for the H_2SO_4 decomposition step for the HyS plant to achieve the same overall plant efficiency. If a more efficient HTGR nuclear plant is used to generate the electricity, the HTGR-powered water electrolysis would have a 30.6% overall LHV efficiency and would only consume 791 kJ of thermal energy per mol H_2 product. This would leave an allowance of 791 kJ – 258 kJ = 533 kJ heat per mol H_2 for the H_2SO_4 decomposition step. A reasonable goal for the HyS plant might be a high-temperature heat requirement for H_2SO_4 decomposition (and auxiliaries) of no more than about 450 kJ/mol H_2. In that case, the HyS plant would be about 25% and 10% more efficient than a water electrolysis plant using conventional and advanced nuclear power plants for electricity production, respectively.

2.3 The bayonet decomposition reactor

One of the most difficult challenges in decomposing sulfuric acid at high temperatures (>800 °C, 1073 K) and pressures (up to 90 bar) is finding a material that can contain the process at the required conditions without significantly corroding or deteriorating, while providing adequate heat transfer characteristics. Silicon carbide (SiC) is among the handful of substances identified so far that meet these requirements. Since SiC is ceramic, it can not be shaped as easily as metal. This greatly complicates the design and fabrication of process vessels and fluid

conduits. A particular concern is making and maintaining sealed joints between individual SiC and SiC-metal components that operate at high temperature and pressure.

As noted above, the two leading thermochemical cycles share the high-temperature decomposition of sulfuric acid as a common step. Responsibility for developing this reaction process for the NHI program belongs to Sandia National Laboratories (SNL), which was initially assigned to do this as part of an international collaboration with General Atomics (GA) and France's Commissariat à l'Energie Atomique (CEA) to build an integrated SI cycle demonstration at GA [13]. The same process should be easily adaptable to the HyS cycle, with minor modifications.

SNL has devised an innovative solution that makes use of readily available SiC shapes and does not have any high-temperature connections [14]. Their bayonet decomposition reactor features internal recuperation and allows all of the connections to be made at relatively low temperatures, where polytetrafluoroethylene (PTFE) and similar materials can be used for seals. The essential elements of SNL's bayonet decomposition reactor are shown in Fig. 3.

In its simplest form, the reactor consists of one closed ended SiC tube co-axially aligned with an open ended SiC tube to form two concentric flow paths. A baffle tube may be included to enhance heat transfer. High-temperature heat is applied externally, except near the open end. Concentrated liquid H_2SO_4 is fed at the open end to the annulus, where it is vaporized before passing through an annular catalyst bed. The decomposition reaction takes place in the catalyst bed, using heat provided by the external heat source. SO_2, O_2, and H_2O vapor product returns through the center and loses its heat to the feed through recuperation. Cooled and partially condensed product exits out the open end into a metal base or manifold at a temperature low

enough (≤ ~250 °C, or 523 K) to allow the use of PTFE seals. Imbedding the open ends of the SiC tubes in a metallic manifold facilitates the transition to metal pipe.

The catalyst for this reactor is being developed by Idaho National Laboratory (INL) as part of the NHI. Metal oxide-supported platinum has been shown to have good activity, but lacks long-term stability and is costly [15]. The focus of the INL work has recently shifted to complex metal oxides, which look more promising [16].

Heat transfer limitations will impose a high surface-to-volume ratio limit, keeping diameters small, so it should be obvious that a single bayonet will not have sufficient capacity for a full-scale reactor. However, it is easy to envision an arrangement in which many bayonets are attached in parallel to a manifolded base plate to achieve the necessary production rate. This would be at least somewhat analogous to the common practice with commercial fixed bed catalytic reactors, in which an endothermic reaction is carried out in parallel in multiple narrow tubes held between two tubesheets, with the heat source on the shell side. Advantages of the bayonet design include internal heat recuperation, the need for low-temperature connections only, corrosion resistance, and low fabrication cost. In fact, SiC bayonets are an off-the-shelf item, since they are used commercially for thermowells[3].

3. Analysis

3.1 Heat requirement for the bayonet decomposition reactor

As noted earlier, if the SDE operates at a cell potential of -0.6 V the balance of the HyS cycle can consume no more than about 450 kJ/mol H_2 of high-temperature heat in order to be

[3] For example, Saint-Gobain Ceramics markets Hexoloy® sintered alpha silicon carbide thermowells that range from 6 to 54 in (0.15 to 1.37 m) in length and from 0.375 to 1.5 in (0.0953 to 0.0381 m) in diameter.

competitive with water electrolysis. Thus, it is important to establish what the heat requirement is for the bayonet reactor.

The heating requirement was determined by means of a pinch analysis. The objective of this analysis was to quantify the high-temperature heating target, which provides a lower limit for the heat input needed to drive the decomposition reaction. The Second Law of Thermodynamics guarantees that the actual heat consumption can only be greater than or equal to the target value.

Since this was a bounding calculation, there was no need to do a detailed heat transfer design. Instead, the assumption was made that the bayonet design was adequate for achieving good heat transfer. This means that the reaction can be accomplished with a practical bayonet length and that reasonable temperature differences can be attained. For this calculation, a 25 °C (25 K) minimum difference between the temperature of the process fluid in the annulus and the temperature of the helium heat transfer medium flowing countercurrently across the bayonet surface was imposed. A smaller, 10 °C (10 K) temperature approach between the annulus and center tube fluids was also used.

The pinch analysis assumed that the process fluid moves through the bayonet reactor in plug flow, and that the catalyst allows the decomposition reaction to proceed to thermodynamic equilibrium at the local pressure, temperature, and composition. An Aspen Plus™ flowsheet model was devised to track the progress of a fluid element as it passes through the reactor, from the inlet, up the annulus and the catalyst bed, down the center tube, and to the outlet. Sufficiently small temperature increments were used (on the order of 10 °C or 10 K) to allow the construction of detailed heating and cooling curves (enthalpy as a function of temperature) for a determination of the heating target.

Aspen Technology, Inc. (AspenTech) provides its licensees an Oleum Data Package for use with Aspen Plus™ that provides accurate representation of H_2SO_4 properties and phase equilibria over the entire concentration range, from 0 through 100% H_2SO_4 to 100% sulfur trioxide (SO_3 or oleum). Unfortunately, the temperature range for this data package extends no higher than 150 °C (423 K), while the pressure is limited to about 2 bar. This limitation was removed by Mathias in work commissioned by General Atomics for modeling the SI cycle [17]. Mathias' work is in the public domain [18].

Mathias split his H_2SO_4 properties model into two temperature ranges. For temperatures below about 300 °C (573 K), he refit AspenTech's oleum model simultaneously to the vapor-liquid equilibrium correlation developed by Gmitro and Vermeulen [19] and to excess enthalpy [20] and heat capacity [21] data for H_2SO_4-H_2O mixtures. Here the underlying Chen Electrolyte-NRTL (ELECNRTL) property method assumes that aqueous H_2SO_4 dissociates to form sulfate and bisulfate anions,

$$H_2SO_4(aq) + H_2O(l) \leftrightarrow H_3O^+ + HSO_4^- \tag{3}$$

$$HSO_4^- + H_2O(l) \leftrightarrow H_3O^+ + SO_4^{2-} \tag{4}$$

The model also includes a vapor phase dissociation equilibrium for H_2SO_4,

$$H_2SO_4(g) \rightarrow H_2O(g) + SO_3(g) \tag{5}$$

At higher temperatures (above 300 °C, or 573 K), the electrolyte model tends to break down, so Mathias replaced the aqueous dissociation equilibria of H_2SO_4 with a nonvolatile complex-forming equilibrium,

$$H_2SO_4(aq) + H_2O(l) \leftrightarrow 2IonPair \tag{6}$$

The postulated complex "IonPair" is assumed to be a molecular component with very low vapor pressure, so the model has no electrolytes. Equation (5) was left unchanged. Mathias fit this

model to the high-temperature, high-pressure data of Wüster [22] as well as to extrapolations of the lower temperature excess enthalpy and heat capacity data. Fig. 4, reproduced from Mathias' report [17], shows that the model matches Wüster's data very well.

For this work, Mathias' H_2SO_4 properties model was modified to take into account solubility data for SO_2 in aqueous H_2SO_4 that were not included in its original development. (SO_2 is treated as a HENRY_COMPS or supercritical component.) The modifications consisted of fitting interaction parameters for SO_2 with other aqueous species to the available data. Furthermore, the optimal transition from the low-temperature, electrolyte to high-temperature, complex-forming model was found to occur at 270 °C (543 K). (The smallest differences between enthalpies calculated using the two methods for a given temperature, pressure, and composition were typically observed around 270 °C, 543 K). Consequently, a switch from one properties model to the other is arbitrarily imposed whenever a stream temperature passes through 270 °C (543 K).

The Aspen Plus™ flowsheet used to set up the decomposition reactor pinch analysis is shown in Fig. 5. Concentrated sulfuric acid is fed at the upper left (stream 1). The blocks along the top row are intended to simulate sequentially the preheating, vaporization, superheating, and decomposition of sulfuric acid as it flows from the bottom of the annulus (left hand side) to the top (right hand side). The blocks along the bottom row simulate the cooling and partial condensing of the effluent from the annular catalyst bed as it flows from top (right hand side) to bottom (left hand side).

Simulation of sulfuric acid decomposition is complicated by the fact that the properties model includes both liquid (equations 3, 4, and 6) and vapor phase (equation 5) equilibrium reactions, and Aspen Plus™ Chemistry models can not account for vapor phase equilibria in the

apparent composition mode. Any reactions involving volatile species on the right hand side must instead be placed in Reactions models, so only those blocks that can explicitly account for chemical reactions (e.g. RCSTR, RGibbs, Radfrac) can correctly represent the high-temperature decomposition of sulfuric acid. That is why the Aspen Plus™ flowsheet in Fig. 5 contains RCSTR and RGibbs blocks instead of the Heater blocks one might reasonably expect to see.

Block HTR1 is a Heater block that uses the low-temperature properties model to calculate the heat required to raise the temperature of the liquid feed (stream 1) to 270 °C (543 K), with the implicit assumption that the equation 5 reaction can be ignored. This is followed by an RCSTR block (HTR2) using the high-temperature properties model to calculate the heat required to vaporize stream 2 while allowing the vapor phase dissociation of H_2SO_4 to H_2O and SO_3 to proceed to equilibrium. A Design Spec is used to adjust the temperature of HTR2 such that the liquid fraction of stream 3 is 2.5% (almost all-vapor). Block HTR3 is identical to HTR2 except that the specified temperature is 10 °C (K) higher, resulting in an all-vapor effluent (stream 4). This arrangement establishes the boiling temperature range for the full pinch analysis model. Block HTR4 is an RGibbs block that uses the high-temperature properties model to calculate the heat required to raise the temperature of all-vapor stream 4 to the inlet temperature of the annular catalyst bed, while allowing the vapor phase dissociation of H_2SO_4 to H_2O and SO_3 to continue toward equilibrium. The SO_3 decomposition reaction (equation 1b) takes place in RGibbs block RXTR, and proceeds to equilibrium simultaneously with equation 5. (The reactions of equations 1b and 5 are not explicitly stated in the RGibbs block specifications, but are implicit in the composition of the individual blocks' Products and Inerts lists.)

Cooling of the decomposition product begins with RGibbs block CLR1, which has specifications identical to those for block HTR4 except that the temperature is just above the dew

point of stream 7. The dew point is determined using a Design Spec in conjunction with RCSTR block CLR2 that adjusts the temperature of CLR2 such that the liquid fraction of stream 8 is 2.5% (almost all-vapor). The other specifications for CLR2 are identical to those for HTR2 and HTR3. A Calculator block sets the temperature of CLR1 10 °C (K) higher than CLR2 in an iterative calculation coupled with the Design Spec, guaranteeing an all-vapor condition for stream 7. This arrangement establishes the condensing temperature range for the full pinch analysis model. RCSTR block CLR3 is identical to CLR2 except that the specified temperature is 270 °C (543 K), allowing transition from the high-temperature to the low-temperature properties model. Block CLR4 is a Heater block that uses the low-temperature properties model to calculate the amount of cooling needed to lower the temperature of the vapor-liquid product (stream 11) to the bayonet outlet temperature, with the implicit assumption that the equation 5 reaction is negligible. A "dummy" RStoic reactor block (DMY) is used to recombine the trace amounts of SO_3 in stream 10 with H_2O to make H_2SO_4, returning the effluent composition to an H_2SO_4 apparent basis.

The full bayonet reactor pinch analysis model contains many more blocks, which result from a subdivision of blocks HTR1, HTR2, HTR4, RXTR, CLR1, CLR3, and CLR4 into multiple, identical blocks in sequential order, with uniform block-to-block temperature increments on the order of 10 °C (10 K), to allow the construction of detailed heating and cooling curves. For example, the liquid feed is heated to 270 °C (543 K) in a series of sixteen heater blocks, each with an outlet temperature that is one-sixteenth of the difference between 270 °C (543 K) and the feed (stream 1) temperature higher than that of the preceding block. Blocks HTR2, HTR4, RXTR, CLR1, and CLR3 are likewise subdivided into 28, 12, 23, 41, and 23 identical blocks, respectively. Block CLR4 is extended to 120 °C (393 K) and subdivided into

fifteen blocks to determine the cooling curve beyond the likely minimum outlet temperature, which is calculated from the pinch analysis.

Results (inlet and outlet temperatures and heat duty for each block) from the full bayonet reactor model were imported into Aspen HX-Net for the pinch analysis. The heating target calculated from the resulting heating and cooling curves represents the minimum high-temperature heat input needed to carry out the decomposition reaction. Fig. 6 illustrates a pinch analysis for the case of 80 wt% H_2SO_4 feed, with the bayonet operating at 86 bar pressure (negligible pressure drop between feed and product) and a peak internal (process) temperature of 870 °C (1143 K). The catalyst bed inlet temperature is assumed to be 675 °C (948 K). This combination of temperatures and pressure would be typical for an advanced, gas-cooled reactor heat source, operating at a 950 °C (1223 K) primary helium coolant outlet temperature and 87-bar outlet pressure, with a 50 °C (50 K) temperature drop across the intermediate heat exchanger [23]. High pressures are needed to minimize the pressure differential between the hot secondary helium coolant flowing outside the bayonet and the interior process stream.

The lower curve in Fig. 6 represents the temperature as a function of heat input (moving from left to right) for the fluid flowing through the annulus, while the upper curve tracks the temperature of the fluid flowing through the central tube of the bayonet as a function of heat removal (moving from right to left). The pinch point represents the closest approach between the temperatures of the two fluids (10 °C or 10 K) flowing countercurrently under optimal heat transfer conditions. The difference between the enthalpies of the two curves at the highest temperature (870 °C or 1143 K), is 328.6 kJ/mol SO_2. This is the heating target, which is the lowest possible high-temperature heat requirement for a bayonet reactor operating at the stated conditions. If all of the SO_2 is delivered to the SDE and consumed to produce H_2, this is

equivalent to 328.6 kJ/mol H_2. Since this number is significantly less than 450 kJ/mol H_2, HyS flowsheets using an SDE operating at a cell potential of -0.6 V coupled to a bayonet decomposition reactor heated by an advanced nuclear heat source have the potential to outperform water electrolysis.

Pinch analyses were performed for a variety of bayonet reactor operating conditions. The results are summarized in Figs. 7 and 8. Fig. 7 plots the high-temperature heat target for H_2SO_4 decomposition over a wide range of feed concentrations (30 to 85%) for three different pressures (57, 70, and 83 bar), while Fig. 8 plots the heat target over a more narrow range of feed concentrations (70 to 85%) for four different pressures (56, 66, 76, and 86 bar). In all cases, the peak process temperature was 870 °C (1143 K), and the catalyst bed inlet temperature was 675 °C (948 K). The lowest heating targets (on the order of 330 kJ/ mol SO_2) were obtained for feed concentrations of 80% at all pressures. Heating targets were below 450 kJ/ mol SO_2 provided the feed concentration was ≥ 60 wt%.

Results of PEM SDE development experiments at SRNL suggest that 50 wt% is the practical upper limit for anolyte acid concentration if a Nafion® or similar sulfonated perfluoroploymer PEM is used. That means the SDE product will need to be concentrated before being fed to the bayonet reactor, or else the high-temperature heat requirement will be impractical (≥ 500 kJ/mol SO_2). Consequently, a HyS process that uses PEM electrolysis in conjunction with a bayonet decomposition reactor will need an acid concentration section, preferably one that can make use of heat recovered from the other flowsheet sections to effect the necessary separation. It will also need a decomposition product handling system to separate and remove O_2 co-product while feeding SO_2 and H_2O to the SDE and recycling unconverted H_2SO_4 back to the bayonet.

3.2 Integrating the bayonet reactor with a PEM SDE

It is assumed that the SDE anolyte product is 50-wt% H_2SO_4 at 100 °C (373 K) and 20 bar, and that it contains unreacted SO_2 as well as traces of O_2. (Higher temperatures give better kinetics, but can't be tolerated by perfluoropolymer PEMs. Higher pressures favor SO_2 solubility, but are limited by SO_2 vapor pressure – two liquid phases could otherwise form in the SDE in some circumstances.) To integrate the SDE with a bayonet reactor, most of the anolyte will need to be recycled. The remaining product stream, containing one mole of H_2SO_4 for each mole of H_2 produced in the SDE, will be passed on. Unreacted SO_2 and trace O_2 will first need to be removed from this stream, along with about one-third (to yield 60 wt% H_2SO_4) to three-quarters (to yield 80 wt% H_2SO_4) of the water content. Similarly, the bayonet product will have to be cooled, unreacted H_2SO_4 recycled, O_2 removed, and the remaining SO_2 and water condensed and combined with recycled, spent anolyte to form fresh anolyte feed.

The simplest way to remove unreacted SO_2 and trace O_2 from the SDE product is to drop the pressure. This requires recompressing the predominantly SO_2 and trace O_2 vapor stream that is out-gassed so that it can be recycled to the SDE feed system. However, the shaft work required is not excessive, and the separation can be made without any heat input.

A variety of methods is available for concentrating the degassed SDE product. All require the expenditure of energy, some more than others. For example, 50% H_2SO_4 at 100 °C (373 K) and 20 bar can be concentrated to 75% H_2SO_4 by simply dropping the pressure to just under 0.05 bar while maintaining the temperature at 100 °C (373 K) requiring just over 169 kJ/mol H_2SO_4 heat input. Water boils off as a separate vapor phase. The pressure could also be maintained at 20 bar and the SDE product heated to 317 °C (590 K) instead to boil off the water.

This would take just over 246 kJ/mol H_2SO_4 heat input. In either case, the heat required is excessive, and would cause the sum of the acid concentration and decomposition step heat duties to exceed the 450-kJ/mol H_2 practical upper limit before even considering the recycled undecomposed acid concentration step. It is clear that a recuperative method is necessary.

Vacuum distillation with recuperative preheating/partial vaporization of the feed streams was chosen to concentrate the SDE product. A two-stage steam ejector can be used to maintain column pressure, while temperatures can be kept high enough to allow use of cooling water in the condenser, yet low enough to allow metallic materials of construction. Water removed in the concentration process can be condensed and recycled to the SDE feed system. The vacuum column bottoms, containing concentrated sulfuric acid, can be easily pumped to the necessary pressure and fed directly to the bayonet reactor.

The bayonet reactor effluent can be readily separated into unreacted H_2SO_4 feed and the SO_2/O_2 product by doing a vapor/liquid split. The acid can be recycled to the vacuum still, while the vapor can be further cooled and let down to the SDE pressure. This will result in a three-phase system: wet liquid SO_2, a saturated solution of SO_2 in H_2O, and wet O_2 gas contaminated with SO_2. The O_2 gas can be scrubbed with the water collected in the concentration process to remove most of the SO_2. The two liquid phases can then be combined with that water and with recycled, spent anolyte to form fresh anolyte feed.

An important consideration is that since the SDE and bayonet reactor already pose significant technological challenges by themselves, the balance of the flowsheet should not introduce additional technical hurdles, but should only use proven technology. This will help give performance projections much greater credibility. The aforementioned flowsheet choices accomplish this goal.

4. Results and discussion

4.1 The PEM SDE / Bayonet Reactor Hybrid Sulfur flowsheet

An Aspen Plus™ flowsheet was prepared that incorporates the elements described in the preceding section. This flowsheet is illustrated in Fig. 9. Stream compositions and conditions are detailed in Table 2. The basis is a 1-kmol/sec H_2 production rate.

While a modification of Mathias' H_2SO_4 properties model worked very well for bayonet decomposition reactor simulations, it was not set up to handle some parts of the HyS flowsheet, particularly those where SO_2 is present as a separate, nonaqueous liquid phase and can no longer be treated as a supercritical component. Furthermore, the need to transition between the low- and high-temperature models for streams that are heated or cooled through 270 °C (543 K) can cause enthalpy mismatches. For these reasons, the flowsheet simulations were done instead using OLI Systems, Inc.'s Mixed Solvent Electrolyte (MSE) model, which has been shown to represent the H_2SO_4-H_2O system very well over its entire composition range and at temperatures as high as 500 °C (773 K) [24]. (The Aspen-OLI interface allows use of the OLI Engine from within Aspen Plus™.) Spot checks of the OLI MSE model's representations of SO_2-H_2O and SO_2-H_2SO_4-H_2O vapor-liquid and liquid-liquid equilibria against the available data showed generally good agreement (e.g. see Figs. 10 [25,26,27] and 11 [28),29,30]).

Returning to the flowsheet, the SDE, block EL-01, is on the left-hand side. Stream 1 is the H_2O feed to the cathode side, while stream 2 is 15.5 wt% SO_2 dissolved in 43.5 wt% H_2SO_4, fed to the anode side. Both streams are assumed to be at 21 bar pressure, and the SDE is assumed to impart a pressure drop of 1 bar due to frictional losses. The composition of stream 2 was set such that the quantity of dissolved SO_2 is just below the saturation point (beyond which a

separate liquid SO_2 phase would form) and that the concentration of H_2SO_4 in the anolyte product following the reaction would be 50% by weight (not including SO_2).

Since a detailed model of the SDE has not yet been developed, it was treated as a "black box" in which the following changes take place:

- A net flux of H_2O from the cathode to the anode (assumed to be 1 kmol H_2O / kmol SO_2 reacted) is imposed. This results from the difference in water activity across the PEM.
- Reaction occurs between SO_2 and H_2O to make H_2SO_4 and H_2 via equation (2) with an assumed SO_2 conversion of 40% (i.e. the anolyte feed contains 150% excess SO_2).
- All of the H_2 product exits the cathode with the remaining water via stream 3.
- All remaining constituents exit the anode via stream 11.
- To simulate no heat lost to the surroundings, the temperatures of streams 3 and 11 are assumed to be identical and are calculated such that the enthalpy change between the feed (1 and 2) and product (3 and 11) streams is equal to the electrical work performed with a cell potential of 0.6 V. (This allows the heat dissipated due to the overpotential to be removed downstream.)
- Streams 3 and 11 are assumed to exit the SDE at a pressure of 20 bar.

The temperature of the SDE (and streams 3 and 11) is maintained at 100 °C (373 K) by adjusting the temperature of anolyte feed stream 2 using heat exchanger HX-06. Experimental evidence for the diffusion of water from the cathode to the anode in a PEM SDE has been provided by Weidner and co-workers [31] at the University of South Carolina (USC). The assumed flux of 1 kmol H_2O / kmol SO_2 reacted is an estimate that needs to be refined with further experiments.

The assumed SO_2 conversion of 40% is a design goal based on experimental results at SRNL and USC. Higher conversion means less material to be recycled, but at the expense of

higher cell potential due to lower average SO_2 concentration at the anode. Conversions in excess of 20% have been routinely achieved in SDE development experiments at SRNL, and over 50% at USC using gaseous SO_2 feed. The optimum value of conversion will be determined by a trade-off between cell potential and recycle effects once the relationship between conversion and cell potential is established.

A mixture of H_2 and H_2O exits the cathode side (stream 3) at 100 °C (373 K) and 20 bar and is cooled by interchange with stream 17 to 77 °C (350 K) in heat exchanger HX-01, maintaining a 10 °C (10 K) minimum temperature difference. The vapor phase (stream 5) is removed in knock-out drum KO-01 and fed to the H_2 Dryer (DR-01), which is cooled to 40 °C (313 K) with cooling water and is assumed to remove all of the H_2O (stream 8). Pure, dry H_2 is produced (stream 6) at 40 °C (313 K) and 20 bar. The "feedstock" H_2O that is to be split into H_2 and O_2 (stream 9) is combined with recycled H_2O (stream 7) and that removed by the dryer (stream 8) and pumped back to the cathode feed by means of the cathode feed pump (PP-01). Since the flux of water across the PEM from the cathode to the anode due to diffusion is assumed to be exactly 1 kmol H_2O / kmol SO_2, this closes the water-splitting material balance.

A detailed design for the H_2 Dryer was not made, and regeneration requirements were not taken into account. Simple cooling from 77 °C to 40 °C (350 K to 313 K) should remove most of the water by condensation; the remainder could be absorbed by a molecular sieve. This simplification is not expected to have a significant impact on cost or energy efficiency.

The anolyte product (stream 11), containing 9.1 wt% unreacted SO_2 dissolved in 50.1 wt% H_2SO_4, is split at SP-01, sending enough H_2SO_4 to decomposition via stream 12 to make all of the SO_2 needed for the SDE. The remainder (representing 80% of the anolyte effluent) is recycled to the anolyte prep tank (TK-01) via stream 48, which is first cooled to 80 °C (353 K)

by interchange with stream 17 in heat exchanger HX-05, maintaining a 10 °C (10 K) minimum temperature difference.

The pressure of the anolyte product is dropped in three stages before being fed to the Vacuum Column (TO-01). Adiabatic throttling valve VV-01 drops the pressure to atmospheric, allowing over 90% of the SO_2 and all but a trace of the dissolved O_2 to be removed in knock-out drum KO-02 via stream 52, along with some H_2O. Next, the pressure is dropped to slightly over 0.3 bar via adiabatic throttling valve VV-02. A steam-driven vacuum ejector (EJ-01) provides the suction needed to maintain vacuum. Nearly 90% of the remaining SO_2 and a little more H_2O are removed in knock-out drum KO-03 via stream 69. Finally, the pressure is dropped to match the feed stage pressure in the Vacuum Column (0.11 bar) by means of adiabatic throttling valve VV-03. The resulting 50.7% H_2SO_4 stream (number 17) is heated and partially vaporized by interchange with six other streams in heat exchanger HX-02, maintaining a 10 °C (10 K) minimum temperature difference with all of them. When fed to the Vacuum Column on equilibrium stage 5, stream 18 is at 94.4 °C (367.6 K) and has a vapor fraction of almost 37%.

The Vacuum Column is maintained at an overhead pressure of 0.09 bar by means of the second-stage steam ejector, EJ-02. The pressure drop from bottom to top is assumed to be 0.04 bar, so the bottoms is at 0.13 bar[4]. TO-01 has 9 equilibrium stages, including a partial condenser (stage 1) and a kettle reboiler (stage 9). The reflux ratio (reflux/distillate) is 0.1, and the distillate vapor fraction is 0.001. A bottoms concentration of 75% H_2SO_4 is achieved by adjusting the distillate rate (to just under 4.4 kmol/sec). Under these conditions, the bottoms is at 122.9 °C (396 K) and requires 75.5 kJ/mol H_2 heating, which can be supplied with a low-pressure steam

[4] Vendor-prepared rating calculations indicate that a column pressure drop as low as 0.02 bar should be possible if FLEXERAMIC® 88 ceramic or FLEXIPAC® HC 2Y metallic structured packing from Koch-Glitsch is used.

utility. The overhead is at 40 °C (313 K) and requires 210.5 kJ/mol H_2 cooling, all of which could be provided using a conventional cooling water system[5].

Bottoms product from the Vacuum Column (stream 19) is 75 wt% H_2SO_4 at 122.9 °C (396 K) and 0.13 bar. It is pumped directly to the Bayonet Reactor (RX-01) by means of pump PP-02, which raises the pressure to 86 bar. A separate simulation (detailed in Section 5 above) was used to establish the minimum high-temperature heating target for RX-01, resulting in the requirement of 340.3 kJ/mol H_2, which would need to be provided by the high-temperature nuclear heat source. The fractional conversion of H_2SO_4 was 48.1%, and the effluent temperature was 254.7 °C (528 K) with a vapor fraction of about 20.4%.

The product of the Bayonet Reactor (stream 21) is separated into its liquid (stream 22) and vapor phase (stream 31) components in knock-out drum KO-04. The pressure of the liquid product is then dropped to 21 bar by means of adiabatic throttling valve VV-04, allowing about 80% of the dissolved SO_2 and 99% of the dissolved O_2 to be removed in knock-out drum KO-05. The remaining liquid (stream 24) is a 59.3 wt% H_2SO_4 solution at 233.4 °C (507 K) that can be recycled to the Vacuum Column. The vapor that was removed (stream 47) contains some of the SO_2 and O_2 products of the decomposition reaction. It is sent to the SO_2 Absorber (TO-02) for separation.

The recycled, unconverted H_2SO_4 stream (number 24) is dropped in pressure before being fed to the Vacuum Column in three stages in a manner identical to the SDE anolyte product. Adiabatic throttling valve VV-05 decreases the pressure to atmospheric, allowing over 99% of the SO_2 and all but a trace of the dissolved O_2 to be removed in knock-out drum KO-06 via stream 54, along with about 22% of the H_2O. Next, the pressure is dropped to slightly over

[5] This may be impossible to achieve in some climates during the summer, since it implies the cooling water supply temperature does not exceed 30 °C (303 K).

0.3 bar via adiabatic throttling valve VV-06. Nearly 99% of the remaining SO_2 and more H_2O are removed in knock-out drum KO-07 via stream 71. Finally, the pressure is dropped to match the feed stage pressure in the Vacuum Column (0.13 bar) by means of adiabatic throttling valve VV-07. The now 67.1 wt% H_2SO_4 stream (number 29) is heated and partially vaporized by interchange with two other streams in heat exchanger HX-03, maintaining a 10 °C (10 K) minimum temperature difference with both. When fed to the Vacuum Column on equilibrium stage 8, stream 30 is at 114.6 °C (387.8 K) and has a vapor fraction of 13.5%.

Hot (254.7 °C, 5278 K) vapor from the Bayonet Reactor (stream 31) is cooled to 40 °C (313 K) and partially condensed in three steps (by heat exchangers HX-04A, HX-04B, and HX-04C), after which it is separated into one vapor and two liquid phases in knock-out KO-08. The lighter liquid phase consists of H_2O with 27.3 wt% dissolved SO_2 and a small amount of O_2. The heavier phase is liquid SO_2 containing 3.7 wt% H_2O and a small amount of O_2. HX-04A is cooled by interchange with the recycled acid feed to the Vacuum Column (HX-03), while HX-04B interchanges with the anolyte product feed to the Vacuum Column (HX-02). HX-04C rejects heat to cooling water. In practice, it would not be necessary to separate the two liquid phases in KO-08, since both are ultimately sent to the Anolyte Prep Tank. However, the split is shown to make the point that separate aqueous and SO_2 phases can and do exist at these conditions.

The vapor and liquid effluents from KO-08 are let down in pressure from 86 bar to 21 bar via adiabatic throttling valves VV-08, VV-09, and VV-10, which leads to further phase changes. The vapor phases are separated from the residual liquids in knock-outs KO-09, KO-10, and KO-11, and fed to the bottom of the SO_2 Absorber, while the liquid phases are sent to the Anolyte Prep Tank.

Returning to the acid concentration part of the flowsheet, the second-stage ejector (EJ-02) effluent (stream 85) is cooled to 40 °C (313 K) with cooling water in heat exchanger HX-12 and the condensate (stream 86) pumped to waste by means of pump PP-09. This helps ensure that any contaminants that may have entered with the steam (stream 84) are purged from the system. The remaining vapors (stream 89) are sent to knock-out KO-14, which is maintained near 0.3 bar by means of the first-stage ejector, EJ-01. KO-14 also receives the partially condensed vapors from knock-outs KO-03 (stream 70) and KO-07 (stream 73), after having first been cooled with cooling water to 40 °C (313 K) by heat exchangers HX-09 and HX-10B . Some of the heat released by condensation (in heat exchanger HX-10A) is transferred by interchange to HX-02. The aqueous phase removed by KO-14 (stream 74) is pumped to the SO_2 Absorber by means of pump PP-07, where it is fed on stage 3.

First-stage ejector (EJ-01) effluent (stream 78) is cooled to 40 °C (313 K) with cooling water in heat exchanger HX-11 and the condensate (stream 79) sent to waste. The remaining vapors (stream 80) are sent to an atmospheric pressure knock-out, KO-12. This knock-out also receives partially condensed vapors from knock-outs KO-02 and KO-06. Vapors removed in knock-out KO-02 (stream 52) are first cooled to 40 °C (313 K) with cooling water by heat exchanger HX-07, while those removed in knock-out KO-06 (stream 54) are cooled to 40 °C (313 K) in a series of three heat exchangers: HX-08A, which drops the temperature to 110.5 °C (384 K) by interchange with HX-03; HX-008B, which further cools to 77 °C (350 K) by interchange with HX-02; and HX-08C, which uses cooling water to achieve an outlet temperature of 40 °C (313 K).

The liquid recovered in knock-out KO-12 (stream 67) is a dilute solution of SO_2 in H_2O (4.8% by weight). It is pumped to the SO_2 Absorber by means of pump PP-06, where it is fed on

stage 5. The vapor removed by the knock-out (stream 58) is a moist SO_2 stream (7.3 mol% H_2O) containing about 0.3 mol% O_2. It needs to be compressed to 21 bar before it can be fed to the bottom of the SO_2 Absorber. This is accomplished with the three-stage SO_2 Recycle Compressor, CO-01, which has intercoolers and knock-outs that cool the outlet of each stage to 40 °C (313 K) and remove any condensate.

The first stage raises the pressure to 2.78 bar. About 5% (by volume) of the feed condenses and is removed as a 12.9% (by weight) solution of SO_2 in H_2O (stream 62) in the first stage intercooler and knock-out. Pump PP-04 is used to send this stream to the Anolyte Prep Tank. The second stage raises the pressure to 7.65 bar. Most of the effluent from this stage condenses in the intercooler and is removed by the knock-out (stream 64) as nearly pure liquid SO_2 containing 0.8% H_2O by weight and a trace of O_2. Pump PP-05 sends this stream to the Anolyte Prep Tank. Partially condensed effluent from the last stage (stream 59) is fed to knock-out KO-13. Of the original feed to CO-01 (stream 58), less than 1% (by volume) remains in the vapor phase (stream 66) and is fed to the bottom of the SO_2 Absorber; a little more than twice that amount is removed as condensate (stream 60) and sent to the Anolyte Prep Tank. Stream 66 is roughly 65% O_2/35% SO_2 (by volume), while stream 60 is 99.9% SO_2 (by weight), with minor amounts of O_2 and H_2O.

The SO_2 Absorber is an eight-equilibrium stage vapor-liquid fractionation device. It operates at 21 bar pressure with an assumed negligible pressure drop. Liquid distillate from the Vacuum Column (stream 81) is fed by means of pump PP-08 to the top stage. This stream is 99.9% H_2O by weight, with 0.1% SO_2 at 40°C (313 K). Effluent from the second-stage ejector knock-out (stream 75), containing 98.7% H_2O by weight, with 1.3% SO_2 at 41 °C (314 K) is fed to stage 3. The first-stage ejector knock-out effluent (stream 68) is routed to stage 5. It contains

95.2% H_2O by weight, with 4.8% SO_2 at 40 °C (313 K). Vapor effluents from five knock-outs and the Anolyte Prep Tank vent are fed to the bottom. SO_2 is scrubbed from the vapor phase as it rises up the Absorber, encountering water with progressively less dissolved SO_2. The overhead product (stream 90) is 98.7% O_2 (by volume) at 41 °C (314 K) and 21 bar, with 0.5% H_2O and 0.8% SO_2. It is fed to the O_2 Dryer (DR-02), where the H_2O and SO_2 are removed (stream 93) and routed to the Anolyte Prep Tank, leaving a pure O_2 product (stream 91) at 40 °C (313 K) and 21 bar. The SO_2 Absorber bottoms stream (92) contains 14.1% (by weight) SO_2 in H_2O at 82 °C (355 K) and 21 bar, with traces of O_2 and H_2SO_4. It is sent to the Anolyte Prep Tank.

As was true for the H_2 Dryer, a detailed design for the O_2 Dryer was not made, and regeneration requirements were not taken into account. Selective absorption of SO_2 and H_2O by a molecular sieve would be the likely mechanism. This simplification is likewise not expected to significantly impact capital cost or energy efficiency.

All of the SO_2 produced by the decomposition of H_2SO_4, as well as that recovered from the SDE anolyte effluent and any liquids end up in the Anolyte Prep Tank. The resulting liquid (stream 51) is a 43.5% H_2SO_4 solution (by weight), containing 15.5% SO_2 at a temperature of 84.7 °C (358 K) and a pressure of 21 bar. This is fed to the SDE anode after adjusting the temperature in heat exchanger HX-06 (by interchange with stream 17 via HX-02) to achieve a 100 °C (373 K) SDE outlet temperature. The anolyte feed (stream 2) temperature is 78.8 °C (352 K).

Make-up sulfuric acid is added to the Anolyte Prep Tank as needed to compensate for SO_2 and H_2O losses due to the ejector blow-downs. (More water is wasted via stream 88, which also contains some SO_2, than enters with streams 77 and 84.) The quantity of make-up needed is

very small (about 0.008 kmol total/kmol H_2 product) and the sulfur content, at 23.6% H_2SO_4 (by weight), corresponds to only about 0.0004 kmol S/kmol H_2 product.

4.2 Flowsheet energy requirements

Heat exchanger specifications are presented in Table 3. Looking at all the entries, heat input is required in only two places: the Bayonet Reactor (RX-01) and the Vacuum Column (TO-01) reboiler. The Bayonet Reactor obviously needs a high-temperature heat source, with heat input of 340.3 kJ/mol H_2. The reboiler, on the other hand, could use low-temperature heat, since it operates in the 100 to 125 °C (373 to 398 K) range. The amount needed is only 75.5 kJ/mol H_2. A grand total of 252.9 kJ/mol H_2 waste heat is rejected to cooling water, over 80% of which occurs in the Vacuum Column condenser. Recuperation is responsible for 130.5 kJ/mol H_2 worth of heating in HX-02 and 31.8 kJ/mol H_2 in HX-03.

A small quantity of steam is also needed to drive the vacuum ejectors (streams 77 and 84, estimated using a one-to-one molar entrainment ratio). The combined amount was calculated at about 0.0277 kmol/sec, which corresponds to a 1.31-kJ/mol H_2 heat duty (from the enthalpy difference between boiler feed water at 40°C, or 313 K, and 7.91-bar steam). This is two orders of magnitude smaller than the Bayonet Reactor duty, so it has little impact on the efficiency calculation. A more rigorous ejector design should be undertaken to confirm the validity of this simplification.

Electric power requirements are detailed in Table 4. A total of 120.9 kJ/mol H_2 electric energy is used in the flowsheet, nearly all of it (115.8 kJ/mol H_2) by the SDE. The SO_2 Recycle Compressor is responsible for most of the rest, about 2.8 kJ/mol H_2. It should be kept in mind that frictional losses due to flow through piping and equipment have been largely ignored, so the

actual pumping requirement will be somewhat higher. If a thermal-to-electric conversion efficiency of 45% is assumed, the total electric power requirement corresponds to a heat input of 268.7 kJ/mol H_2.

Adding together the high- and low-temperature heat requirements, the total heat supplied to the process is 417.1 kJ/mol H_2. This meets the ≤450 kJ/mol H_2 goal discussed in Section 2.2. When the thermal equivalent of the power requirement is added, this flowsheet consumes a total of 685.8 kJ/mol H_2, which compares favorably with HTGR-powered water electrolysis at 791 kJ/mol H_2. The comparison is made more favorable if it is acknowledged that a significant portion of the heat can be supplied by another source. The 76.8 kJ/mol H_2 heat duty needed by the Vacuum Column reboiler and the steam ejectors could be supplied by a low-pressure steam utility with a non-HTGR primary source. In that case, the quantity of HTGR heat needed by this flowsheet would be only 609 kJ/mol H_2 (including the thermal energy needed for electricity production).

4.3 Discussion

The flowsheet presented above combines a PEM SDE with a bayonet reactor, using only proven chemical process technology. If the SDE and the high-temperature decomposition reactor perform as projected (-0.6 V cell potential, 40% conversion, 50 wt% H_2SO_4 product; 25 °C or K minimum temperature difference between He coolant and process stream, 10 °C or K minimum temperature difference between process streams, adequate heat transfer characteristics) the flowsheet process will produce H_2 and O_2 from H_2O while consuming 340.3 kJ/mol H_2 high-temperature heat, 75.5 kJ/mol H_2 low-temperature heat, 1.31 kJ/mol H_2 low-pressure steam, and 120.9 kJ/mol H_2 electric power. Should the ultimate source of all of this energy be an HTGR

(process heat as well as electricity at 45% conversion efficiency), the net thermal efficiency would be 35.3% (LHV basis, or 41.7%, HHV basis). This is significantly more efficient than alkaline electrolysis (4.8 kWh/Nm^3 H_2) or PEM electrolysis (4.4 kWh/Nm^3 H_2) coupled with HTGR power (28.1% or 30.7%, LHV basis, respectively).

In reality, the efficiency difference may be even larger than it seems. HTGR electric power (at least initially) will likely be more expensive than conventional BWR/PWR power. Passive safety constraints limit individual HTGR reactors to no more than about 600 MW_{th} in size, while the lower-temperature BWR/PWR reactors can be significantly larger [32][6]. Economies of scale help to make the otherwise less efficient BWR/PWR power less expensive. Eventually, standardized design, factory production, and higher efficiency may overcome this limitation, but not until a number of HTGR plants have been built. Consequently, water electrolysis is initially more likely to be powered by electricity made using water-cooled reactors, which can not achieve the temperatures needed for the H_2SO_4 decomposition step in sulfur cycles. This means the net thermal efficiency (including electric power generation) for H_2 production by water electrolysis will actually be approximately 22.4%.

It also means that HTGRs will initially likely be used primarily for process heat, and that the HyS SDE will probably be powered by electricity from the grid. In that case, the net thermal efficiency for the HyS flowsheet process will be 30.9% (LHV basis), assuming grid power is produced by water-cooled reactors. This compares very favorably with the 22.4% efficiency calculated for water electrolysis.

In any event, it is the unit cost of H_2 production ($/kg H_2) that will ultimately determine whether the HyS process will be commercialized. If water can be split into H_2 and O_2 more

[6] The European Pressurized Water Reactor (EPR) under construction in Finland is rated at 4,300 MW_{th} and 1,600 MW_e [32].

economically by this method than by simple electrolysis or other competing process, then HyS plants will be the preferred choice for H_2 production using nuclear power. A detailed estimate of the unit cost of H_2 production using the HyS process will be the subject of a future paper.

One additional caveat needs to be kept in mind when considering these results. Moving hot, pressurized helium through ductwork and heat exchangers requires a significant expenditure of energy. As noted in a DOE Nuclear Energy Research Initiative (NERI) study published in 2006 [33], the primary and secondary loop circulators for a 600-MW_{th} HTGR coupled with a Sulfur-Iodine cycle process would require on the order of 25 MW_e electric power. Comparable power requirements would be expected for a HyS process. While the work performed on the helium heat transfer fluid is eventually recovered in the form of heat, the conversion loss that occurs with electric power generation imposes an additional energy penalty that should be included in the efficiency calculation. However, the actual power requirement depends on the design of the nuclear heat source, which was not part of this work. The detailed H_2 production cost estimate being prepared for a future paper will include the HTGR as well as the helium heat transfer loops.

Finally, 252.9 kJ/mol H_2 waste heat is rejected to cooling water. This too will require some expenditure of electric energy (to pump water to and from the cooling tower), but the amount should be much smaller than that needed for the reactor heat transfer loops. The cooling water system will also be included in the future paper.

4.4 Assumptions

The flowsheet presented above relies on a series of assumptions for its predicted performance. While these have been clearly stated, a brief discussion as to their implications is in order.

Perhaps the most critical assumption is that the properties models used for flowsheet calculations accurately represent the H_2SO_4 - H_2O - SO_3 - SO_2 - O_2 system. This premise is valid for the OLI MSE H_2SO_4 - H_2O - SO_3 model [24]. Mathias' high-temperature extension of AspenTech's Oleum Data Package [17] also provides a sufficiently good representation of H_2SO_4 - H_2O - SO_3 properties. Accurate models for the solubility/miscibility of SO_2 in/with mixtures of H_2SO_4 and H_2O, however, are still lacking. Figs. 10 and 11 show that while the OLI MSE model gives generally good agreement with the available data for this ternary, the fit could be much better. As for O_2, little attention has been paid to its solubility in H_2SO_4 or SO_2. These shortcomings, while not serious enough to have a material effect on the outcome of this work, will need to be addressed in future HyS process development efforts.

Another crucial assumption is that heat transfer can be achieved as needed in the high-temperature decomposition reactor in order to achieve the specified approach temperatures. Removing heat transfer from consideration allows a pinch analysis to establish the reactor performance limit dictated by thermodynamics, i.e. determine the high-temperature heating target. This is useful in determining the bounds for reactor operating conditions and performance. Results demonstrate that the bayonet concept has the potential to decompose sulfuric acid efficiently enough for a practical HyS process. Furthermore, the selected approach temperatures are consistent with good engineering practice. A coupled heat transfer analysis still needs to be performed, however, to verify that the concept can be made to work using a hot

helium heat transfer medium and with practical reactor dimensions, and to provide a design basis for a capital cost estimate.

Flowsheet calculations also assume that the high-temperature decomposition reaction proceeds to thermodynamic equilibrium. If conversion were to fall short of equilibrium, the recycle rate of unconverted acid would increase, raising the Vacuum Column reboiler duty by a small amount. The decomposition process is catalytic, so it is not unreasonable to expect that a sufficient volume of catalyst could allow the reaction to approach equilibrium. Consequently, this is not an unreasonable assumption for a bounding calculation. The reader should be aware that the actual conversion in the bayonet reactor could be somewhat less than that shown.

Absent a phenomenological model of the electrolyzer, SDE operation has been characterized using development performance targets, i.e. the SDE is assumed to operate at a fixed cell potential of -0.6 V, with a fixed SO_2 conversion of 40%, and at a fixed 50-wt% H_2SO_4 product composition. If these targets can not be met, the efficiency advantage of HyS over water electrolysis will be diminished. The conversion target should be the easiest to achieve, while the cell potential will likely be the hardest. An SDE unit operation model that can be incorporated into the flowsheet and that relates these cell performance measures to input parameters would help determine how much these targets can be relaxed. Such a model will need to be built for future development efforts.

The heat duties calculated for blocks HX-02 and HX-03 represent target values as determined by pinch analysis. A practical heat exchanger network will need to be designed for the heat recovery scheme used by these blocks before a capital cost can be estimated for the flowsheet.

The flowsheet ignores piping and vessel pressure drops. These will add to the actual power requirement (due to the need for pumping), but the increase should be small enough to disregard for now. Furthermore, a uniform 10 °C (10 K) minimum temperature difference for process heat exchange is assumed throughout. Optimal minimum temperature differences will vary from exchanger to exchanger, but this is a reasonable starting point for the conceptual design of a process in which energy recovery is at a premium. One significant exception was the assumption of a 25 °C/K minimum temperature difference between the process fluid in the bayonet reactor and the helium heating stream.

Finally, the assumption that process streams can be cooled to 40 °C (313 K) with cooling water implies that cooling water is available year-round at 30 °C (303 K) or lower temperature. This may be somewhat geographically limiting, but it allows the Vacuum Column to be operated without a refrigerated condenser. The effect of increasing the summer cooling water temperature above 30 °C (303 K) will need to be evaluated for operation in hot climates.

5. Summary and Conclusions

The HyS cycle splits H_2O into H_2 and O_2 by combining the high-temperature, endothermic, catalytic decomposition of H_2SO_4 into H_2O, SO_2, and O_2 with SO_2-depolarized electrolysis that regenerates H_2SO_4. A HyS process flowsheet has been developed for use with electric power and high-temperature heat sources that combines the PEM SDE technology being developed at SRNL with bayonet reactor H_2SO_4 decomposition technology being developed at SNL. Conventional water electrolysis was proposed as a benchmark against which to compare this HyS cycle. If electricity is available at a 45% heat-to-power conversion efficiency (e.g. HTGR with Brayton cycle PCU), water electrolysis could be used to make H_2 for a net energy

consumption of perhaps as little as 791 kJ/mol H_2. Development goals for SRNL's PEM SDE include sustained operation at a cell potential of -0.6 V, which was shown to be equivalent to a 258-kJ/mol H_2 primary energy source. This leaves a margin of 791 kJ –258 kJ = 533 kJ heat per mol H_2 product for the H_2SO_4 decomposition step in order to match the water electrolysis efficiency. A goal of ≤450 kJ/mol H_2 was established to provide an edge.

A pinch analysis was used to establish high-temperature heating targets for the decomposition reactor as a function of pressure and H_2SO_4 feed concentration. Results of the analysis showed that heating targets were below 450 kJ/ mol SO_2 for feed concentration ≥ 60 wt% and that increasing pressure decreases the target. This requires that the SDE product with its maximum concentration of 50 wt% be concentrated before being fed to the bayonet reactor to meet the high-temperature heat requirement goal.

Vacuum distillation with recuperative preheating/partial vaporization of the feed streams and using a two-stage steam ejector was chosen to concentrate the SDE product. Temperatures could be kept high enough to allow use of cooling water in the condenser, yet low enough to allow metallic materials of construction. Only proven process technology was utilized, leaving the SDE and the bayonet reactor as the only major components that need development.

The resulting flowsheet, illustrated in Fig. 9, and with stream and equipment performance data tabulated in Tables 2 through 4, requires 340.3 kJ/mol H_2 high-temperature heat, 75.5 kJ/mol H_2 low-temperature heat, 1.31 kJ/mol H_2 low-pressure steam, and 120.9 kJ/mol H_2 electric power. (If a 45% heat-to-power conversion efficiency is assumed, the electric power corresponds to a primary energy input of 268.7 kJ/mol H_2.) Adding together the heat requirements and the thermal equivalent of the power requirement, it consumes a total of 685.8 kJ/mol H_2, which compares favorably with HTGR-powered electrolysis at 791 kJ/mol H_2. When

conventional nuclear reactors are assumed to be the source of electric power, the HyS process has an even larger advantage over water electrolysis (783 kJ/mol H_2 versus 1,080 kJ/mol H_2, respectively).

Based on this result, the HyS cycle should be competitive with water electrolysis as a means of producing H_2 by water-splitting on a massive scale. It is a necessary prerequisite for commercializing the HyS cycle, that its projected H_2 production cost be lower than that attainable with competing technologies, especially conventional water electrolysis. For a more definitive determination, a detailed economic analysis will be needed, including the cost of building and operating the coupled nuclear heat source. This will be the subject of a future study, which will quantify the cost of H_2 production ($/kg H_2). It is hoped that the detailed process flowsheet design and efficiency estimates presented here will contribute to a better understanding of the current status and future promise of the HyS cycle as a potential major component of a Hydrogen Economy.

Acknowledgements

This work was performed under DOE Contract No. DE-AC09-96SR18500. Funding was provided by DOE-NE under the NHI program. Mr. Carl Sink was the program manager and Dr. Bob Evans (National Renewable Energy Laboratory) provided technical program direction. Their support is acknowledged and greatly appreciated. Helpful interactions with Dr. Paul M. Mathias (formerly with AspenTech, now with Fluor Corp.), Dr. David F. McLaughlin and Dr. Edward J. Lahoda (both Westinghouse Electric Co.), Mr. Charles O. Bolthrunis (Shaw Stone & Webster), and Prof. John W. Weidner (USC) are also gratefully acknowledged.

References

1. The Hydrogen Economy; Opportunities, Costs, Barriers, and R&D Needs. Washington, DC: National Academy of Engineering, 2004.

2. U.S. Department of Energy, Energy Information Administration. Annual Energy Outlook 2008. Report No. DOE/EIA-0383(2008). http://www.eia.doe.gov/oiaf/aeo/, May 27, 2008.

3. Brecher LE, Wu CK. Electrolytic decomposition of water. Westinghouse Electric Corp., US Patent No. 3888750, 1975.

4. Farbman GH. The conceptual design of an integrated nuclear-hydrogen production plant using the sulfur cycle water decomposition system. NASA Contractor Report, NASA-CR-134976, 1976.

5. Lu PWT, Ammon RL, Parker GH. A study on the electrolysis of sulfur dioxide and water for the sulfur cycle hydrogen production process. NASA Contractor Report, NASA-CR-163517, 1980.

6. Parker GH. Solar thermal hydrogen production process. Final Report from Westinghouse Electric Corp. to US DOE, DOE/ET/20608-1, 1983.

7. Brecher LE, Spewock S, Warde CJ. The Westinghouse Sulfur Cycle for the thermochemical decomposition of water. Int J Hydrogen Energy 1977;2(1):7-15.

8. Bard AJ, Parsons R, Jordan J. Standard Potentials in Aqueous Solutions. New York: Marcel-Dekker, 1985.

9. Bratsch SG. Standard Electrode Potentials and Temperature Coefficients in Water at 298.15K. J Phys Chem Ref Data 1989;18:1-21.

10. Lu PWT, Garcia ER, Ammon RL. Recent developments in the technology of sulphur dioxide depolarized electrolysis. J Appl Electrochem 1981;11:347-355.

11. Norsk Hydro Electrolysers AS. High Pressure Electrolysers: 10–60 Nm^3/h. http://www4.hydro.com/electrolysers/en/products/range/high_pressure_electrolyser/, February 25, 2008.

12. Norsk Hydro Electrolysers AS. Product development–the shape of things to come. http://www4.hydro.com/electrolysers/en/products/product_development/, February 25, 2008.

13. International Nuclear Energy Research Initiative, 2006 Annual Report. DOE/NE-131. Washington, DC: United States Department of Energy, 2007. p. 113.

14. Parma EJ, Vernon ME, Gelbard F, Moore RC, Stone HBJ, Pickard PS. Modeling the Sulfuric Acid Decomposition Section for Hydrogen Production. Proc, 2007 Int Topical Mtg on Safety and Technol of Nucl Hydrogen Prodn, Control, & Mgmt, Boston, MA, Jun 24-28, 2007: 154-160.

15. Ginosar DM, Glenn AW, Petkovic LM, Burch KC. Stability of supported platinum sulfuric acid decomposition catalysts for use in thermochemical water splitting cycles. Int J Hydrogen Energy 2007;32(4):482-488.

16. Ginosar DM, Rollins HW, Petkovic LM, Burch KC, Rush MJ. High-temperature sulfuric acid decomposition over complex metal oxide catalysts. Int J Hydrogen Energy 2008 (submitted for publication).

17. Mathias PM. General Atomics and Sandia National Laboratories; Modeling the Sulfur-Iodine Cycle; Aspen Plus™ Building Blocks and Simulation Models. Final Report from Aspen Technology, Inc. to General Atomics, Oct 24 2002.

18. Brown LC et al. High Efficiency Generation of Hydrogen Fuels Using Nuclear Power. Final Technical Report for the period August 1, 1999 through September 30, 2002, from General Atomics Corp. to US DOE, GA–A24285, Jun 2003, Appendix C.

19. Gmitro JI, Vermeulen T. Vapor-Liquid Equilibrium for Aqueous Sulfuric Acid. AIChE J 1964;10:740.

20. Kim SH, Roth M. Enthalpies of Dilution and Excess Molar Enthalpies of an Aqueous Solution of Sulfuric Acid. J Chem Eng Data 2001;46:138-143.

21. Fasullo OT. Sulfuric Acid: Use and Handling. New York: McGraw-Hill, 1965.

22. Wüster G, p, v, T – und Dampfdruckmessungen zur Bestimmung Thermodynamischer Eigenschaften Starker Elektrolyte bei Erhöhtem Druck. doctoral dissertation, RWTH-Aachen 1979.

23. Verfondern K (ed.). Nuclear Energy for Hydrogen Production. Jülich, Germany: Forschungszentrum Jülich GmbH, 2007.

24. Wang P, Anderko A, Springer RD, Young RD. Modeling phase equilibria and speciation in mixed-solvent electrolyte systems: II. Liquid–liquid equilibria and properties of associating electrolyte solutions J Molec Liquids 2006;125:37-44.

25. Miles FD, Fenton J. The solubility of sulfur dioxide in sulfuric acid. J Chem Soc 1920;117:59-61.

26. Kuznetsov DA. Study of the equilibrium pressures of sulfur dioxide over water and aqueous solutions of sulfuric acid (transl.). Zh Khim Prom (USSR.) 1941;18(22):3-7.

27. Miles FD, Carson T. Solubility of sulfur dioxide in fuming sulfuric acid. J Chem Soc 1946:786-90.

28. Maass CE, Maass O. Sulfur dioxide and its aqueous solutions. I. Analytical methods, vapor density and vapor pressure of sulfur dioxide. Vapor pressure and concentrations of the solutions. J Am Chem Soc 1928;50(5):1352-1368.

29. Spall BC. Phase equilibriums in the system sulfur dioxide-water from 25-300°. Can J Chem Engr 1963;41:79-83.

30. van Berkum JG, Diepen GAM. Phase equilibriums in sulfur dioxide + water: the sulfur dioxide gas hydrate, two liquid phases, and the gas phase in the temperature range 273 to 400 K and at pressures up to 400 MPa. J Chem Thermodynamics 1979;11:317-334.

31. Staser J, Ramasamy RP, Sivasubramanian P, Weidner JW. Effect of Water on the Electrochemical Oxidation of Gas-Phase SO_2 in a PEM Electrolyzer for H_2 Production. Electrochem Solid-State Lett 2007;10:E17-E19.

32. Areva NP. Olkiluoto 3, EPR – facts and figures. http://www.ol3.areva-np.com/project/facts.htm. May 29, 2008.

33. Summers WA. Centralized Hydrogen Production from Nuclear Power: Infrastructure Analysis and Test-Case Design Study – Final Project Report, Phase B Test-Case Preconceptual Design, Savannah River National Laboratory Report No. WSRC-MS-2005-00693, Rev. 0, Apr 28 2006.

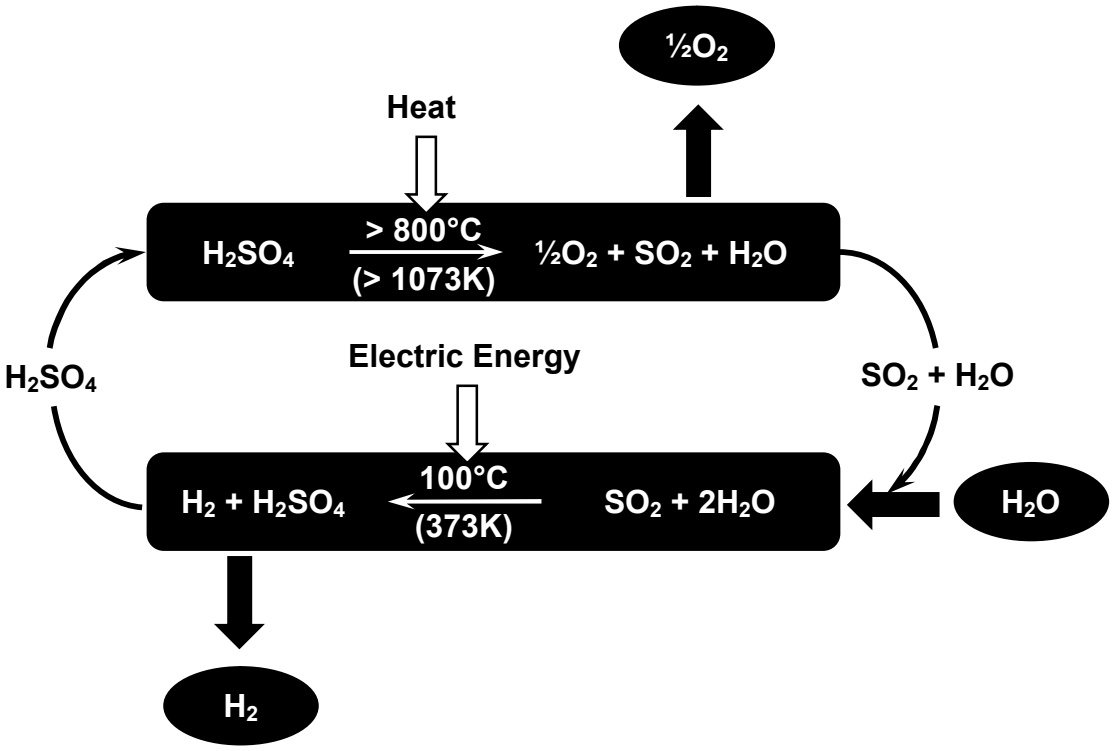
½O2
Heat
H2SO4
> 800°C
(> 1073K)
½O2 + SO2 + H2O
Electric Energy
H2SO4
SO2 + H2O
H2 + H2SO4
100°C
(373K)
SO2 + 2H2O
H2O
H2

Figure 1

The Hybrid Sulfur (HyS) cycle

Maximilian B. Gorensek

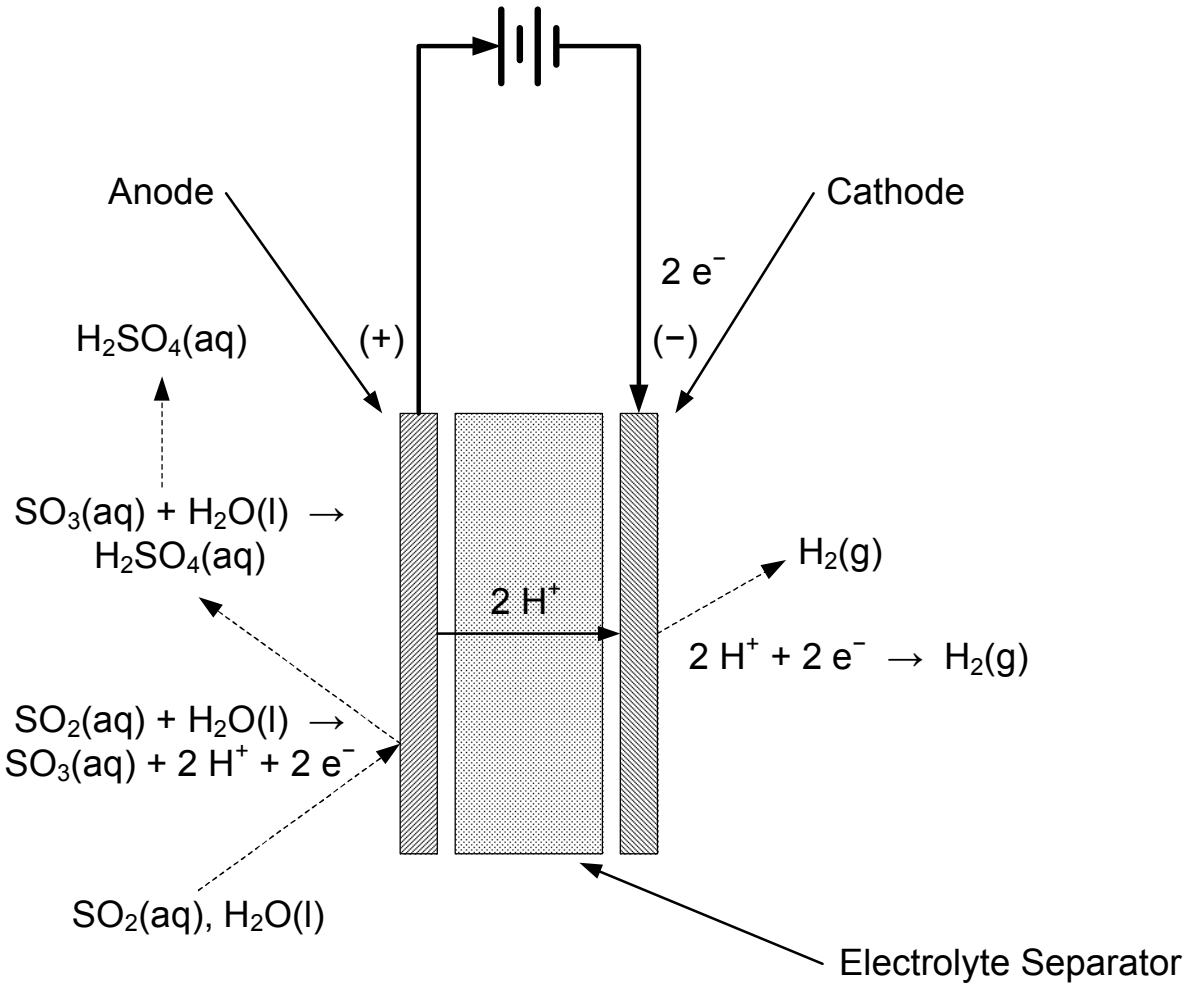
Anode
Cathode
2 e⁻
H2SO4(aq)
(+)
(−)
SO3(aq) + H2O(l) → H2SO4(aq)
H2(g)
2 H+
2 H+ + 2 e⁻ → H2(g)
SO2(aq) + H2O(l) → SO3(aq) + 2 H+ + 2 e⁻
SO2(aq), H2O(l)
Electrolyte Separator

Figure 2

Schematic diagram of an SO_2-depolarized electrolyzer

Maximilian B. Gorensek

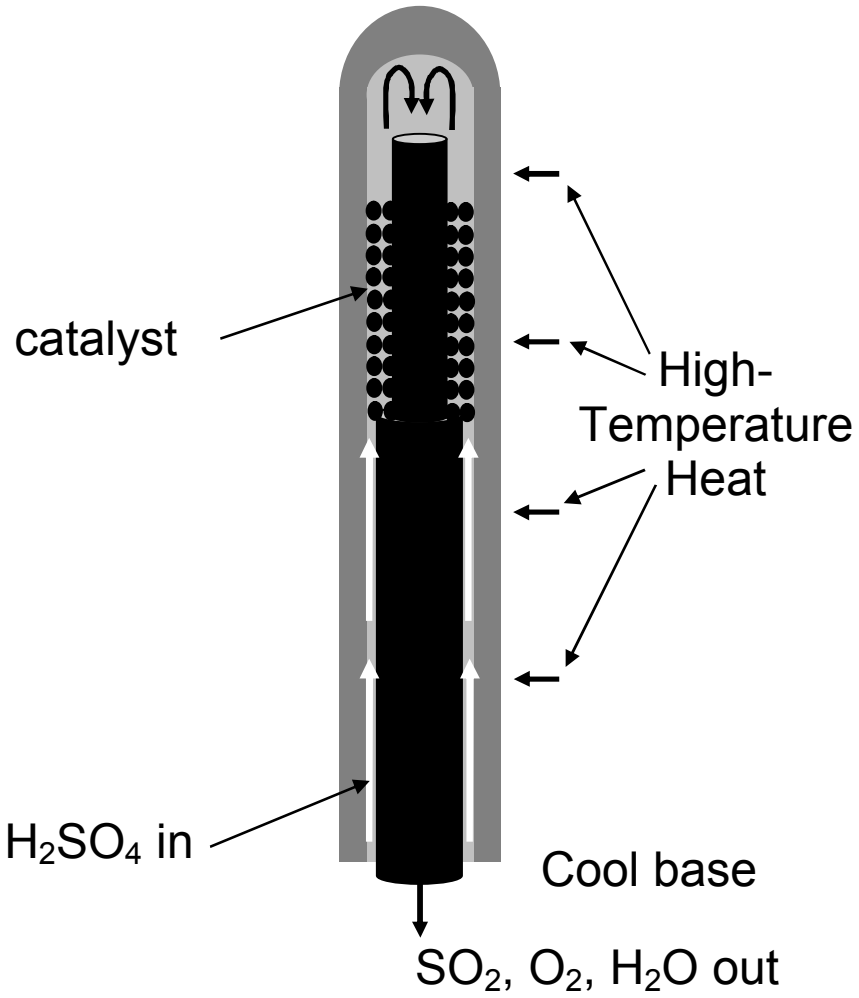
catalyst
High-
Temperature
Heat
H_2SO_4 in
Cool base
SO_2, O_2, H_2O out

Figure 3

Schematic diagram of the SNL bayonet decomposition reactor

Maximilian B. Gorensek

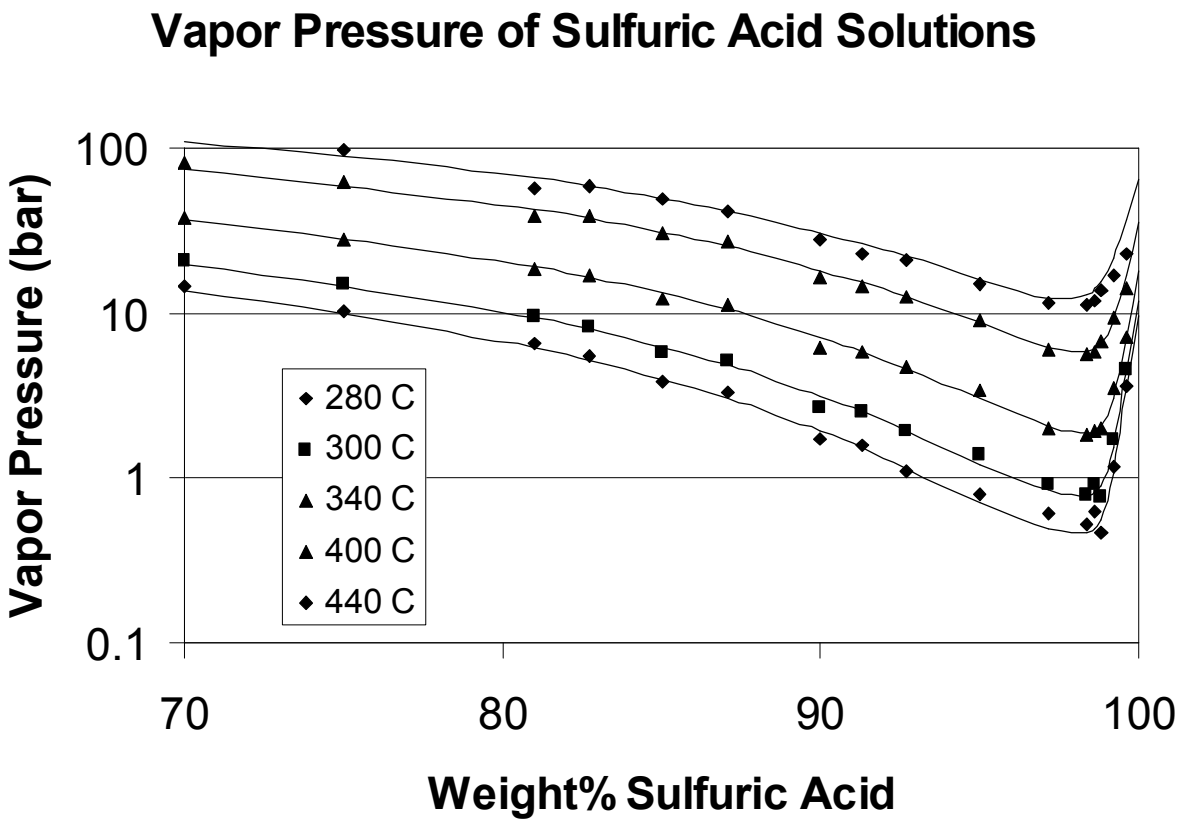
Vapor Pressure of Sulfuric Acid Solutions
Vapor Pressure (bar)
100
10
1
0.1
70
80
90
100
Weight% Sulfuric Acid
280 C
300 C
340 C
400 C
440 C

Figure 4

Vapor pressure of sulfuric acid solutions at high temperature – comparison of Mathias model with data of Wüster

Maximilian B. Gorensek

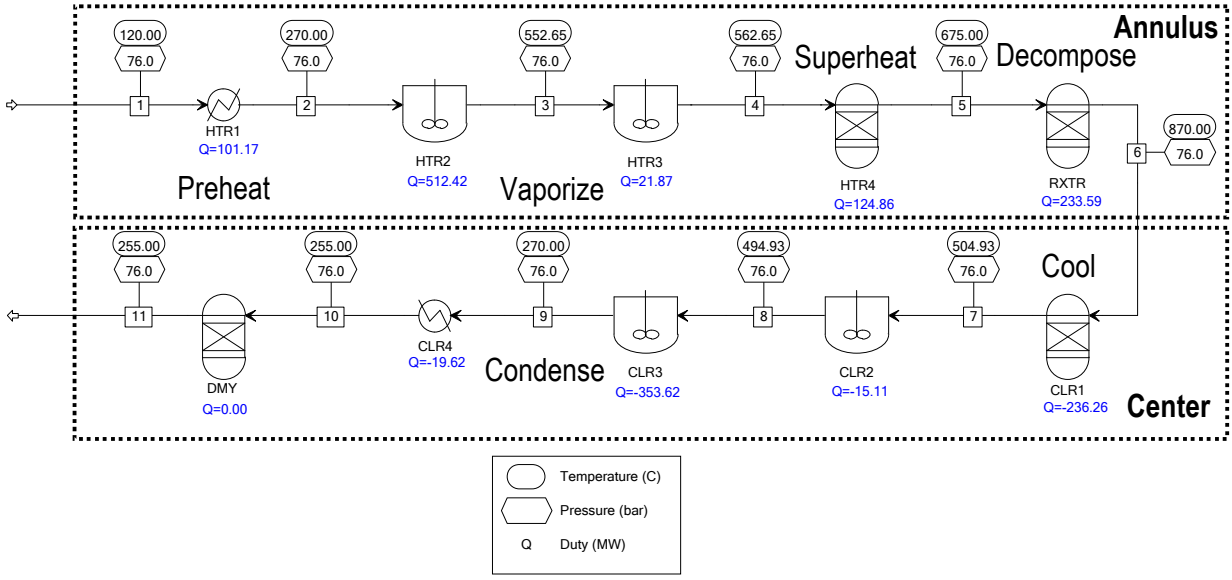
Annulus
120.00
76.0
1
HTR1
Q=101.17
270.00
76.0
2
Preheat
HTR2
Q=512.42
552.65
76.0
3
Vaporize
HTR3
Q=21.87
562.65
76.0
4
Superheat
HTR4
Q=124.86
675.00
76.0
5
Decompose
RXTR
Q=233.59
6
870.00
76.0
Cool
504.93
76.0
7
CLR1
Q=-236.26
494.93
76.0
8
CLR2
Q=-15.11
270.00
76.0
9
Condense
CLR3
Q=-353.62
CLR4
Q=-19.62
255.00
76.0
10
255.00
76.0
11
DMY
Q=0.00
Center
Temperature (C)
Pressure (bar)
Q Duty (MW)

Figure 5

Aspen Plus™ high temperature decomposition reactor pinch analysis set-up flowsheet

Maximilian B. Gorensek

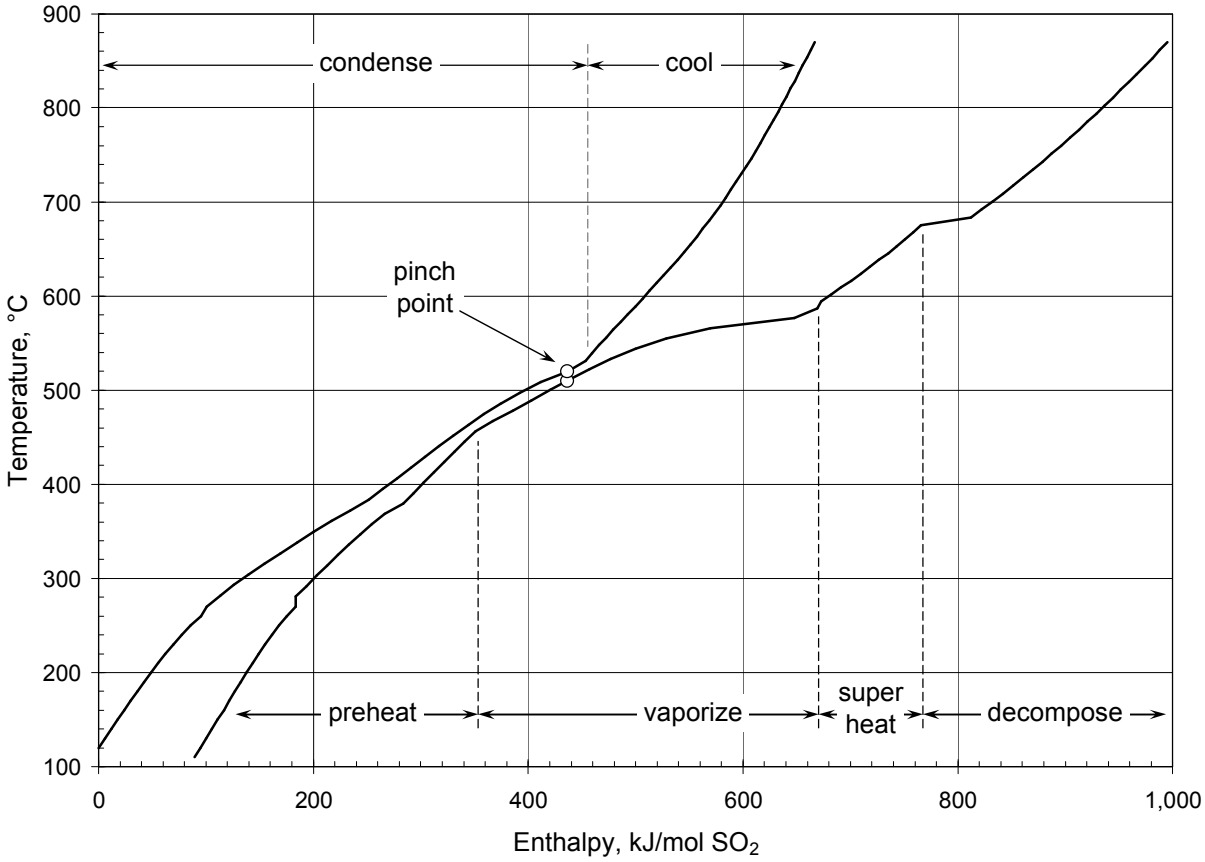
condense
cool
pinch
point
preheat
vaporize
super
heat
decompose
Temperature, °C
Enthalpy, kJ/mol SO_2
900
800
700
600
500
400
300
200
100
0
200
400
600
800
1,000

Figure 6

Bayonet Reactor heating and cooling curves – 80% H_2SO_4 feed, 86-bar pressure, 870 °C (1143 K) peak process temperature, 675 °C (948 K) catalyst bed inlet temperature

Maximilian B. Gorensek

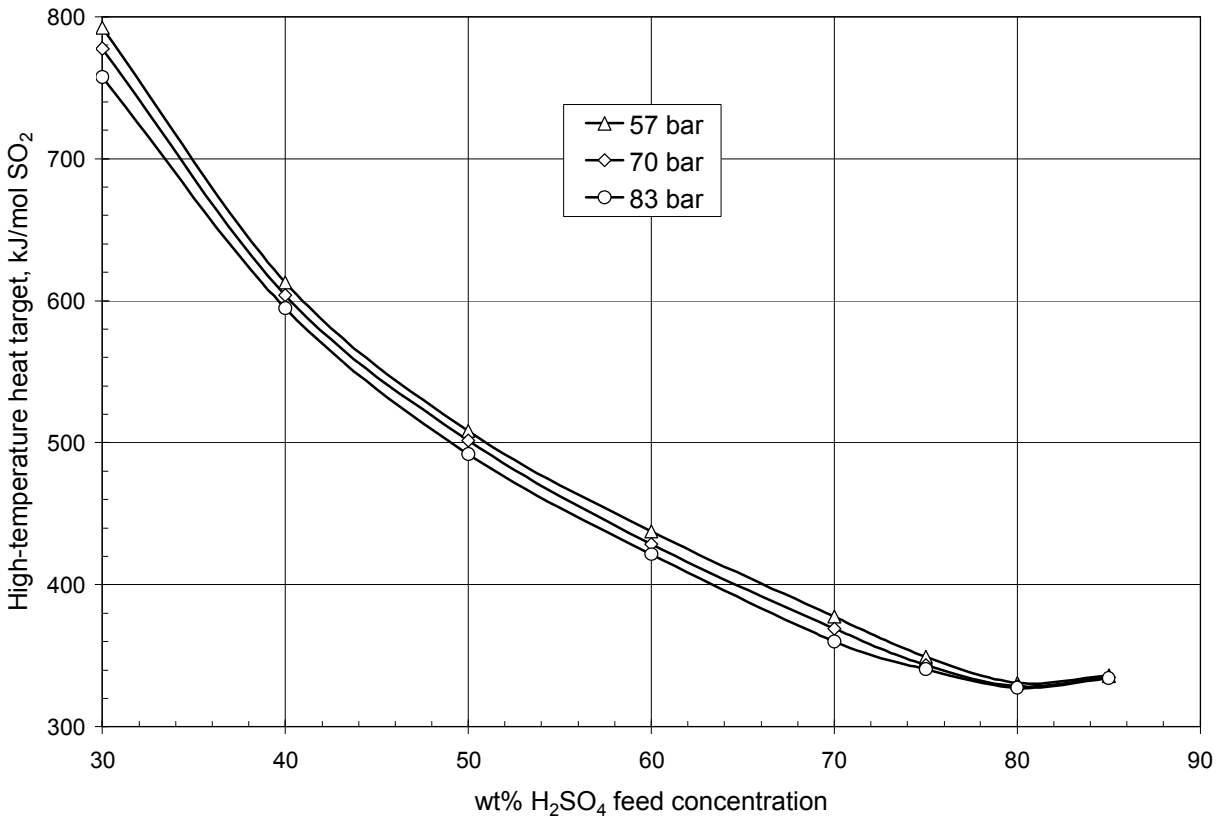
800
700
600
500
400
300
30
40
50
60
70
80
90
High-temperature heat target, kJ/mol SO2
wt% H2SO4 feed concentration
57 bar
70 bar
83 bar

Figure 7

High-temperature heat requirement for H_2SO_4 decomposition as a function of feed concentration (30 to 85%) at three different pressures, 870 °C (1143 K) peak process temperature, 675 °C (948 K) catalyst bed inlet temperature

Maximilian B. Gorensek

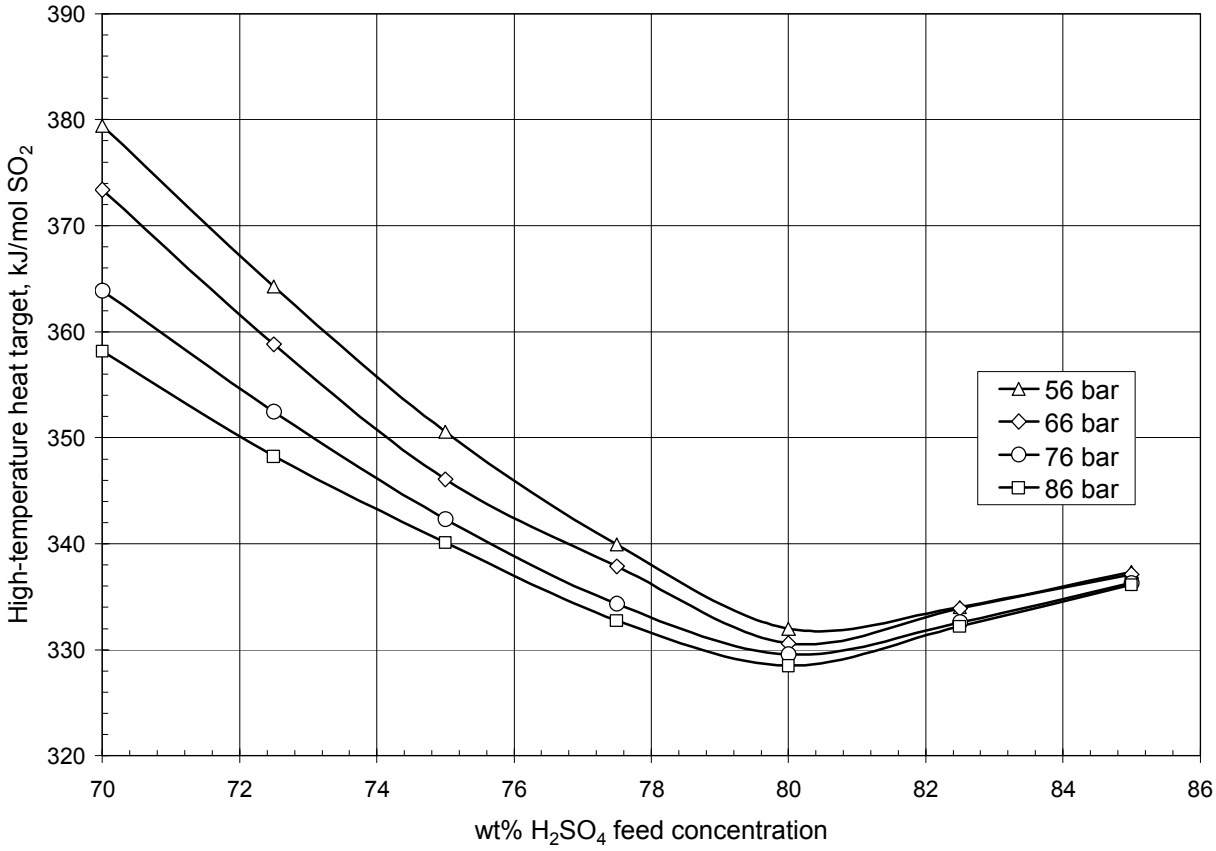
390
380
370
360
350
340
330
320
70
72
74
76
78
80
82
84
86
High-temperature heat target, kJ/mol SO2
wt% H2SO4 feed concentration
56 bar
66 bar
76 bar
86 bar

Figure 8

High-temperature heat requirement for H_2SO_4 decomposition as a function of feed concentration (70 to 85%) at four different pressures, 870 °C (1143 K) peak process temperature, 675 °C (948 K) catalyst bed inlet temperature

Maximilian B. Gorensek

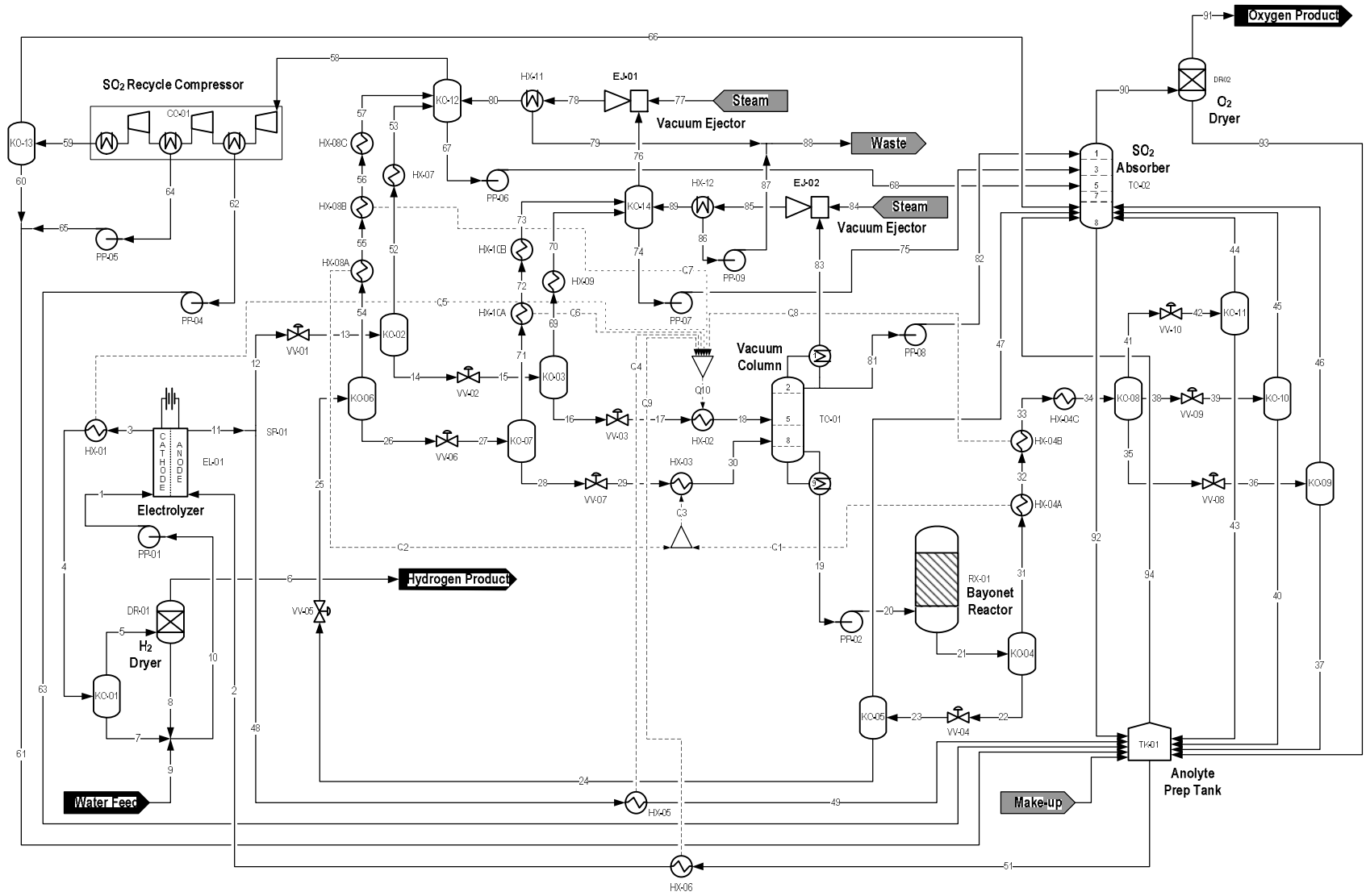
SO_2 Recycle Compressor
CO-01
KO-13
KO-12
HX-11
EJ-01
Steam
Vacuum Ejector
Waste
HX-08C
HX-07
PP-06
HX-08B
HX-12
EJ-02
Steam
Vacuum Ejector
KO-14
PP-09
PP-05
HX-08A
HX-10B
HX-09
PP-04
HX-10A
PP-07
VV-01
KO-02
VV-02
KO-03
Vacuum Column
PP-08
KO-06
Q10
TC-01
HX-01
CATHODE
ANODE
EL-01
SP-01
Electrolyzer
VV-03
HX-02
HX-04C
HX-04B
HX-04A
VV-06
KO-07
HX-03
VV-07
PP-01
Hydrogen Product
VV-05
DR-01
H_2 Dryer
KO-01
RX-01
Bayonet Reactor
PP-02
KO-04
KO-05
VV-04
Water Feed
HX-05
HX-06
Make-up
TK-01
Anolyte Prep Tank
Oxygen Product
DR-02
O_2 Dryer
SO_2 Absorber
TC-02
KO-11
VV-10
KO-08
VV-09
KO-10
VV-08
KO-09

Figure 9

Hybrid Sulfur flowsheet using a PEM SDE and a bayonet decomposition reactor

Maximilian B. Gorensek

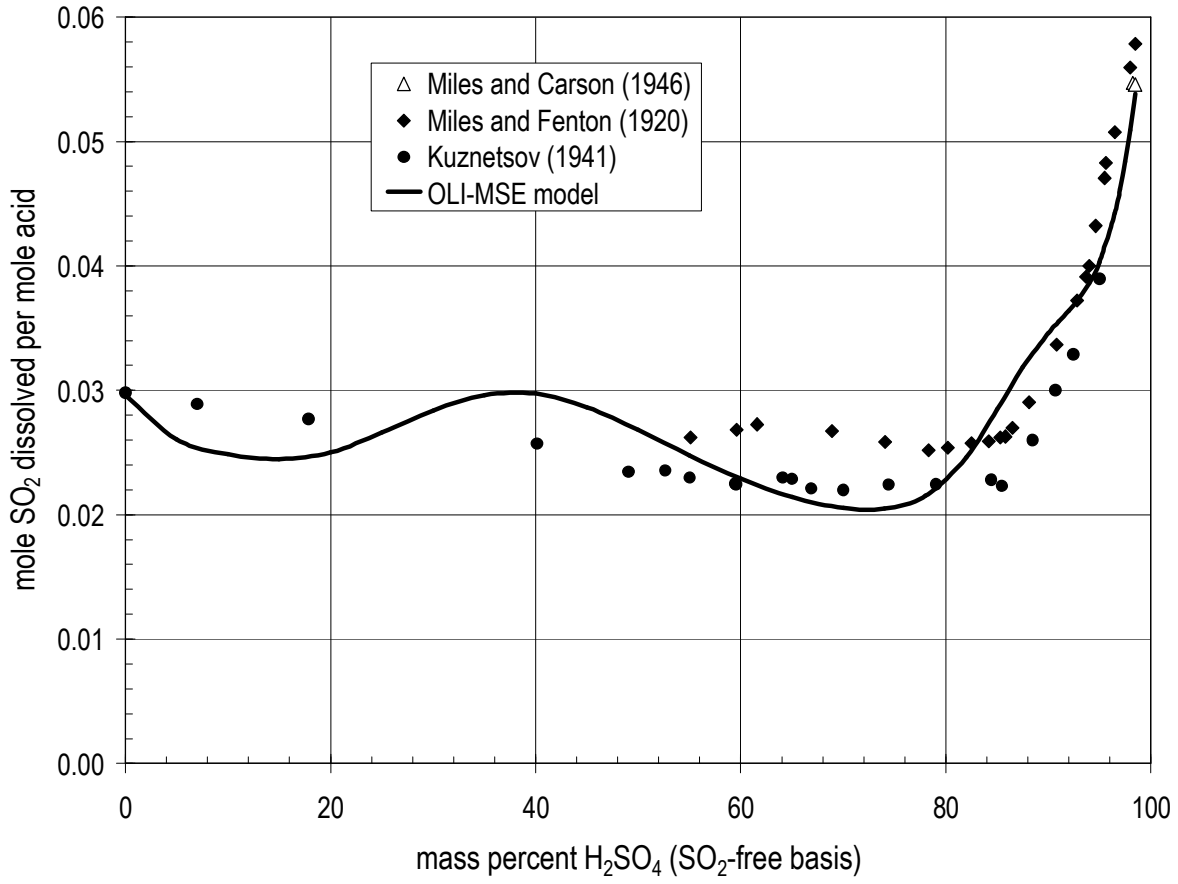
Miles and Carson (1946)
Miles and Fenton (1920)
Kuznetsov (1941)
OLI-MSE model
mole SO2 dissolved per mole acid
mass percent H2SO4 (SO2-free basis)
0.06
0.05
0.04
0.03
0.02
0.01
0.00
0
20
40
60
80
100

Figure 10

Solubility of SO_2 in sulfuric acid at 1.013-bar partial pressure – comparison of OLI MSE model with data of Miles and Carson, Kuznetsov, and Miles and Fenton

Maximilian B. Gorensek

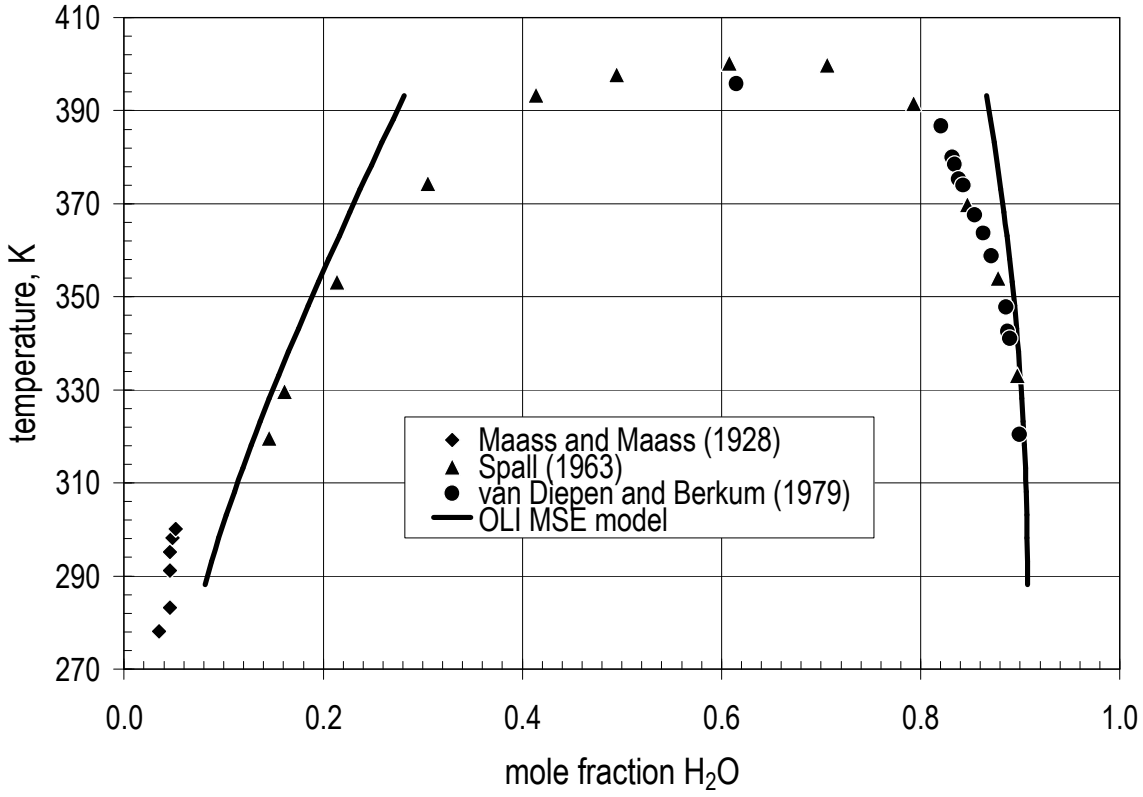
410
390
370
350
330
310
290
270
temperature, K
0.0
0.2
0.4
0.6
0.8
1.0
mole fraction H_2O
Maass and Maass (1928)
Spall (1963)
van Diepen and Berkum (1979)
OLI MSE model

Figure 11

Liquid-liquid phase equilibrium in the SO_2-H_2O system – comparison of OLI MSE model with data of Maass and Maass, Spall, and van Diepen and Berkum

Maximilian B. Gorensek

Table 1

Energy requirement allowances for HyS process

	BWR/PWR Nuclear Power Plant	HTGR Nuclear Power Plant
Thermal-to-electric conversion efficiency, %	33	45
Water electrolysis efficiency (LHV), %	68	68
Nuclear-electrolysis plant efficiency (LHV), %	22.4	30.6
Thermal energy requirement, kJ/mol H_2	1,080	791
HyS SDE cell voltage, V	-0.6	-0.6
Electricity demand, kJ_e/mol H_2	116	116
Thermal equivalent of electricity, kJ_{th}/mol H_2	352	258
Heat available for HyS high-temperature H_2SO_4 decomposition, kJ/mol H_2		
For same efficiency as water electrolysis	728	533
+ 10% efficiency over water electrolysis	630	461
+ 25% efficiency over water electrolysis	512	375
+ 33% efficiency over water electrolysis	460	337
+ 50% efficiency over water electrolysis	368	269

Table 2

Hybrid Sulfur flowsheet stream table

Stream	Molar flow rates, kmol/sec						Temperature,		Pressure,	Phase
ID	H_2O	H_2SO_4	SO_2	O_2	H_2	Total	°C	K	bar	
1	10	0	0	0	0.00235	10.0024	73.20	346.35	21	L
2	27.4794	3.88405	2.5	0.00527	0	37.7528	78.77	351.92	21	L
3	9	0	0	0	1.00235	10.0024	100.00	373.15	20	L + V
4	9	0	0	0	1.00235	10.0024	76.96	350.11	20	L + V
5	0.02185	0	0	0	1.00004	1.02189	76.96	350.11	20	V
6	0	0	0	0	1.00004	1.00004	40.00	313.15	20	V
7	8.97815	0	0	0	0.00231	8.98046	76.96	350.11	20	L
8	0.02185	0	0	0	0	0.02185	40.00	313.15	20	L
9	1	0	0	0	0	1	40.00	313.15	20	L
10	10	0	0	0	0.00231	10.0023	73.19	346.34	20	L
11	26.4794	4.88405	1.5	0.00527	0	37.7528	100.00	373.15	20	L + V
12	5.42394	1.00043	0.30725	0.00108	0	7.73314	100.00	373.15	20	L + V
13	5.42394	1.00043	0.30725	0.00108	0	7.73314	84.08	357.23	1.01325	L + V
14	5.33174	1.00043	0.02004	3.9E-07	0	7.35265	84.08	357.23	1.01325	L
15	5.33174	1.00043	0.02004	3.9E-07	0	7.35265	80.38	353.53	0.30198	L + V
16	5.29406	1.00043	0.00263	2.9E-10	0	7.29756	80.38	353.53	0.30198	L
17	5.29406	1.00043	0.00263	2.9E-10	0	7.29756	66.96	340.11	0.11	L + V
18	5.29406	1.00043	0.00263	2.9E-10	0	7.29756	94.41	367.56	0.11	L + V
19	3.7702	2.07782	6.7E-12	2E-21	0	7.92584	122.87	396.02	0.13	L
20	3.7702	2.07782	6.7E-12	0	0	7.92584	123.63	396.78	86	L
21	4.77063	1.07739	1.00043	0.50021	0	8.42605	254.70	527.85	86	L + V
22	4.30695	1.07739	0.23587	0.00844	0	6.70604	254.70	527.85	86	L
23	4.30695	1.07739	0.23587	0.00844	0	6.70604	233.42	506.57	21	L + V
24	4.03002	1.07739	0.04733	8.9E-05	0	6.23222	233.42	506.57	21	L
25	4.03002	1.07739	0.04733	8.9E-05	0	6.23222	147.33	420.48	1.01325	L + V
26	3.13019	1.07739	0.00035	1.4E-08	0	5.28532	147.33	420.48	1.01325	L
27	3.13019	1.07739	0.00035	1.4E-08	0	5.28532	118.57	391.72	0.30198	L + V
28	2.87261	1.07739	3.7E-06	2.4E-12	0	5.02739	118.57	391.72	0.30198	L
29	2.87261	1.07739	3.7E-06	2.4E-12	0	5.02739	100.50	373.65	0.13	L + V
30	2.87261	1.07739	3.7E-06	2.4E-12	0	5.02739	114.62	387.77	0.13	L + V
31	0.46368	5.5E-06	0.76455	0.49177	0	1.72001	254.70	527.85	86	V
32	0.46368	5.5E-06	0.76455	0.49177	0	1.72002	110.50	383.65	86	L + V
33	0.46368	5.5E-06	0.76455	0.49177	0	1.72002	76.96	350.11	86	L + V
34	0.46368	5.5E-06	0.76455	0.49177	0	1.72002	40.00	313.15	86	L + V
35	0.08967	1.8E-07	0.65507	0.00123	0	0.74597	40.00	313.15	86	L
36	0.08967	1.8E-07	0.65507	0.00123	0	0.74597	41.78	314.93	21	L + V
37	0.08966	1.8E-07	0.65459	0.00025	0	0.74451	41.78	314.93	21	L

38	0.37282	5.3E-06	0.03946	0.00066	0	0.41296	40.00	313.15	86	L
39	0.37282	5.3E-06	0.03946	0.00066	0	0.41296	40.99	314.14	21	L + V
40	0.37282	5.3E-06	0.03922	0.00014	0	0.41218	40.99	314.14	21	L
41	0.00119	0	0.07002	0.48988	0	0.56109	40.00	313.15	86	V
42	0.00119	0	0.07002	0.48988	0	0.56109	15.50	288.65	21	L + V
43	0.0006	0	4.7E-05	3.8E-07	0	0.00065	15.50	288.65	21	L
44	0.00059	0	0.06997	0.48988	0	0.56044	15.50	288.65	21	V
45	3.5E-06	4.3E-26	0.00025	0.00052	0	0.00077	40.99	314.14	21	V
46	6.9E-06	1E-25	0.00048	0.00098	0	0.00146	41.78	314.93	21	V
47	0.27692	1.3E-06	0.18854	0.00835	0	0.47382	233.42	506.57	21	V
48	21.0554	3.88362	1.19275	0.00419	0	30.0196	100.00	373.15	20	L + V
49	21.0554	3.88362	1.19275	0.00419	0	30.0196	80.00	353.15	20	L
50	21.0554	3.88362	1.19275	0.00419	0	30.0196	80.01	353.16	21	L
51	27.4794	3.88405	2.5	0.00524	0	37.7527	84.71	357.86	21	L
52	0.0922	2E-11	0.28721	0.00108	0	0.38049	84.08	357.23	1.01325	V
53	0.0922	2E-11	0.28721	0.00108	0	0.38049	40.00	313.15	1.01325	L + V
54	0.89983	6.6E-07	0.04698	8.9E-05	0	0.9469	147.33	420.48	1.01325	V
55	0.89983	6.6E-07	0.04698	8.9E-05	0	0.9469	110.50	383.65	1.01325	L + V
56	0.89983	6.6E-07	0.04698	8.9E-05	0	0.9469	76.96	350.11	1.01325	L + V
57	0.89983	6.6E-07	0.04698	8.9E-05	0	0.9469	40.00	313.15	1.01325	L + V
58	0.02674	2.3E-24	0.33759	0.00117	0	0.3655	40.00	313.15	1.01325	V
59	1.9E-05	0	0.00541	0.00116	0	0.00659	40.00	313.15	21	L + V
60	1.9E-05	0	0.0048	1.2E-06	0	0.00482	40.00	313.15	21	L
61	0.00936	0	0.33626	1E-05	0	0.34562	41.20	314.35	21	L
62	0.01738	0	0.00073	3.5E-09	0	0.01811	40.00	313.15	2.78324	L
63	0.01738	0	0.00073	3.5E-09	0	0.01811	41.11	314.26	21	L
64	0.00934	0	0.33146	9.2E-06	0	0.3408	40.00	313.15	7.64513	L
65	0.00934	0	0.33146	9.2E-06	0	0.3408	41.22	314.37	21	L
66	3.2E-07	0	0.00061	0.00116	0	0.00177	40.00	313.15	21	V
67	0.96665	6.6E-07	0.01365	6.1E-08	0	0.9803	40.00	313.15	1.01325	L
68	0.96665	6.6E-07	0.01365	6.1E-08	0	0.9803	40.31	313.46	21	L
69	0.03768	6.4E-12	0.01741	3.9E-07	0	0.0551	80.38	353.53	0.30198	V
70	0.03768	6.4E-12	0.01741	3.9E-07	0	0.0551	40.00	313.15	0.30198	L + V
71	0.25758	1E-07	0.00035	1.4E-08	0	0.25793	118.57	391.72	0.30198	V
72	0.25758	1E-07	0.00035	1.4E-08	0	0.25793	76.96	350.11	0.30198	L + V
73	0.25758	1E-07	0.00035	1.4E-08	0	0.25793	40.00	313.15	0.30198	L
74	0.28961	1E-07	0.00106	2.8E-11	0	0.29067	40.61	313.76	0.30198	L
75	0.28961	1E-07	0.00106	2.8E-11	0	0.29067	41.14	314.29	21	L
76	0.0059	1.2E-25	0.01745	4.1E-07	0	0.02335	40.61	313.76	0.30198	V
77	0.02335	0	0	0	0	0.02335	169.99	443.14	7.91	L + V
78	0.02925	0	0.01745	4.1E-07	0	0.0467	93.77	366.92	1.01325	V
79	0.0279	0	0.0004	1.2E-11	0	0.0283	40.00	313.15	1.01325	L

80	0.00135	0	0.01706	4.1E-07	0	0.0184	40.00	313.15	1.01325	V
81	4.39285	6.9E-35	0.00185	4.9E-13	0	4.3947	40.02	313.17	0.09	L
82	4.39285	0	0.00185	4.9E-13	0	4.3947	40.21	313.36	21	L
83	0.00361	5.2E-35	0.00079	3E-10	0	0.0044	40.02	313.17	0.09	V
84	0.0044	0	0	0	0	0.0044	169.99	443.14	7.91	L + V
85	0.00801	0	0.00079	3E-10	0	0.0088	95.05	368.20	0.30198	V
86	0.00777	0	2.9E-05	1.3E-14	0	0.0078	40.00	313.15	0.30198	L
87	0.00777	0	2.9E-05	1.3E-14	0	0.0078	40.04	313.19	1.01325	L
88	0.03567	0	0.00042	1.2E-11	0	0.03609	40.03	313.18	1.01325	L
89	0.00025	0	0.00076	3E-10	0	0.001	40.00	313.15	0.30198	V
90	0.00228	1.4E-34	0.00413	0.50024	0	0.50665	41.12	314.27	21	V
91	0	0	0	0.50024	0	0.50024	40.00	313.15	21	V
92	5.92438	2.1E-06	0.27327	0.00116	0	6.19882	82.33	355.48	21	L
93	0.00228	0	0.00413	0	0	0.00641	40.00	313.15	21	L
94	2.9E-05	7.6E-16	0.00098	0.00051	0	0.00152	84.71	357.86	21	V
MAKE UP	0.00749	0.00042	0	0	0	0.00834	40.00	313.15	21	L

Table 3

Hybrid Sulfur flowsheet heat exchangers

Block ID	Duty, MW_{th}	Temperature, °C (K)		Heat Exchanged With:
		Inlet	Outlet	
CO-01/Stage 1 Cooler	-2.290	138.02 (411.2)	40.0 (313)	Cooling Water
CO-01/Stage 2 Cooler	-9.109	137.79 (410.9)	40.0 (313)	Cooling Water
CO-01/Stage 3 Cooler	-0.132	143.76 (416.9)	40.0 (313)	Cooling Water
DR-01	-2.045	76.96 (350.1)	40.0 (313)	Cooling Water
DR-02	-0.197	41.12 (314.3)	40.0 (313)	Cooling Water
HX-01	-17.688	100.00 (373.0)	76.96 (350.1)	HX-02
HX-02	130.486	66.96 (340.1)	94.41 (367.6)	HX-01, HX-04B, HX-05, HX-06, HX08B, HX-10A
HX-03	31.777	100.50 (373.7)	114.62 (387.8)	HX-04A, HX-08A
HX-04A	-30.543	254.70 (527.9)	110.50 (383.7)	HX-03
HX-04B	-8.400	110.50 (383.7)	76.96 (350.1)	HX-02
HX-04C	-6.243	76.96 (350.1)	40.0 (313)	Cooling Water
HX-05	-47.903	100.00 (373.0)	80.00 (353.0)	HX-02
HX-06	-18.686	84.71 (357.9)	78.77 (351.9)	HX-02
HX-07	-3.702	84.08 (357.2)	40.0 (313)	Cooling Water
HX-08A	-1.234	147.33 (420.5)	110.50 (383.7)	HX-03
HX-08B	-37.440	110.50 (383.7)	76.96 (350.1)	HX-02
HX-08C	-4.021	76.96 (350.1)	40.0 (313)	Cooling Water
HX-09	-1.476	80.38 (353.5)	40.0 (313)	Cooling Water
HX-10A	-0.368	118.57 (391.7)	76.96 (350.1)	HX-02
HX-10B	-11.503	76.96 (350.1)	40.0 (313)	Cooling Water
HX-11	-1.310	93.77 (366.9)	40.0 (313)	Cooling Water
HX-12	-0.354	95.05 (368.2)	40.0 (313)	Cooling Water
RX-01	340.280	123.63 (396.8)	254.70 (527.9)	High-Temp. Source
TO-01 Reboiler	75.482	102.74 (375.9)	122.87 (396.0)	Low-Temp. Source
TO-01 Condenser	-210.542	44.80 (318.0)	40.0 (313)	Cooling Water

Table 4

Hybrid Sulfur flowsheet electrolyzers, pumps, and compressors

Block ID	Work, MW_e
EL-01	115.782
CO-01/Stage 1	1.464
CO-01/Stage 2	1.357
CO-01/Stage 3	0.025
PP-01	0.022
PP-02	1.836
PP-03	0.071
PP-04	0.002
PP-05	0.028
PP-06	0.055
PP-07	0.021
PP-08	0.212
PP-09	0.00003